

Electromagnetic waves interaction with various metallic nanomaterials

Michael Giersig



Department Physics
Institute of Experimental Physics
e-mail: giersig@physik.fu-berlin.de



XLVIII Zakopane School of Physics
breaking frontiers: submicron structures in physics and biology

May 20th - 25th, 2013
Zakopane, Poland

Light Scattering

The scattering of light was first studied in a careful manner by Tyndall in 1859

A major step to explain the phenomenon was taken in 1871 by Rayleigh.

The electric polarisation induced in an atom or a molecule by the electromagnetic field is proportional to ω^2 and the field radiated by such induced oscillating dipoles then becomes proportional to ω^4 .

Rayleigh thus found that the molecular scattering by blue light is many times more than that by red light and so explained the blue colour of the sky as the result of scattering from the air molecules.

When the wavelength of light becomes comparable to the size of the scattering particles, like dust particles, the mutual interference from the scattering by the different portions of the dust particle become important and this is called Mie scattering.

- For spherical simple metal nanoparticles
- Generalized Kohn's theorem

$$\omega = \omega_p / \sqrt{3}$$

L. Brey, N.F. Johnson, and B.I. Halperin, Phys. Rev. B40,10647 (1989)
P. Bakshi, D.A. Broido and K. Kempa, Phys. Rev. B42,7416 (1990)

Gustav Mie, 1908



Fabrication of nanomaterial's: application in electronics

Solar Cell

Photonic

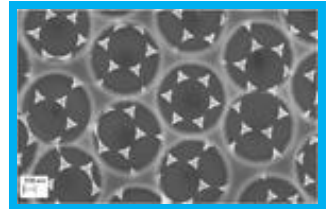
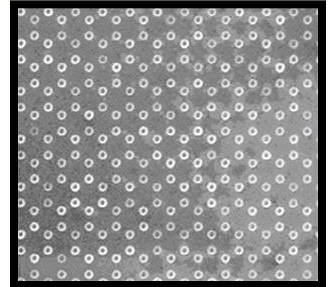
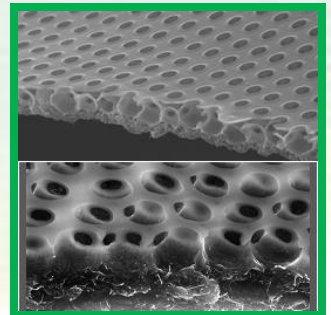
Memory devices

Detection devices

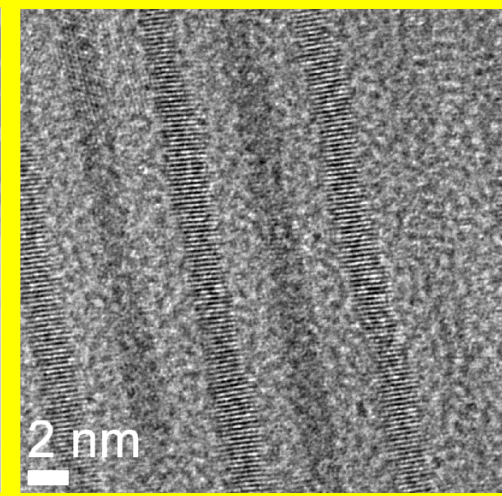
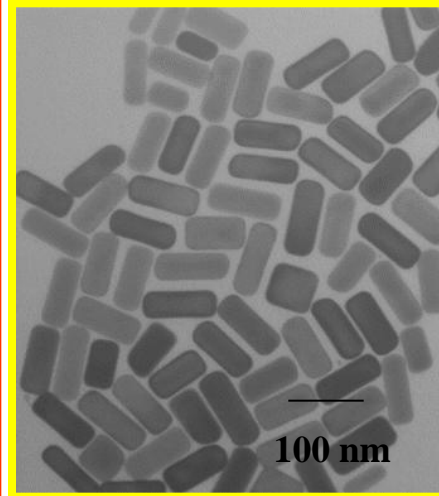
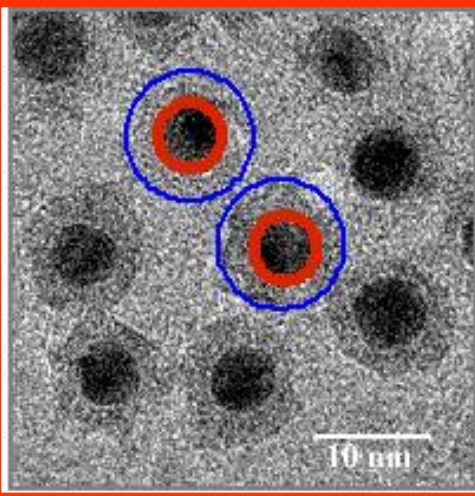
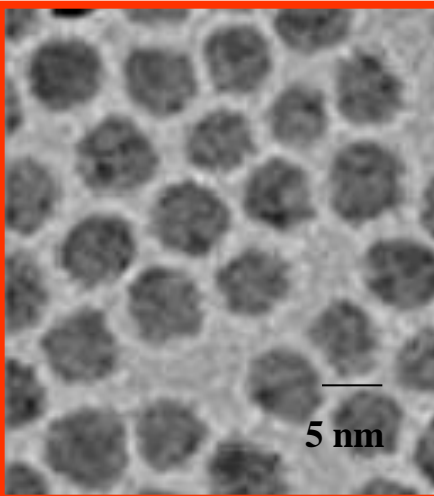
Nano Materials:

antenna, dots, tubes, 2-D and 3-D
rods, rings, photonic crystals,
Hybrides

semiconductor: CdTe, CdS, ZnO
metallic: Au, Ag, Pt
magnetic: Co, Fe₃O₄, Ni
Graphene, carbon SWCNT, MWCNT
Polymer

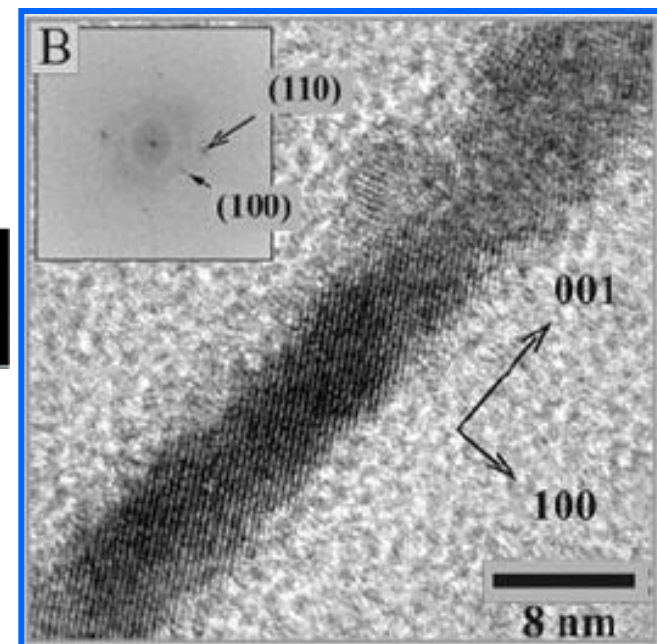
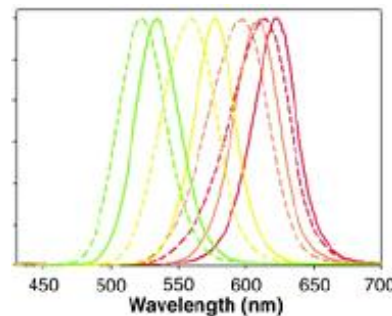
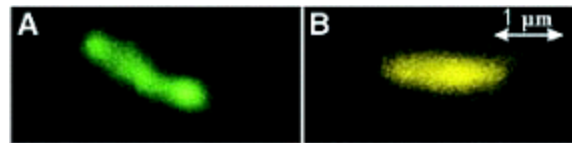
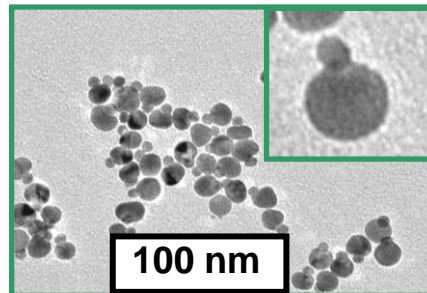
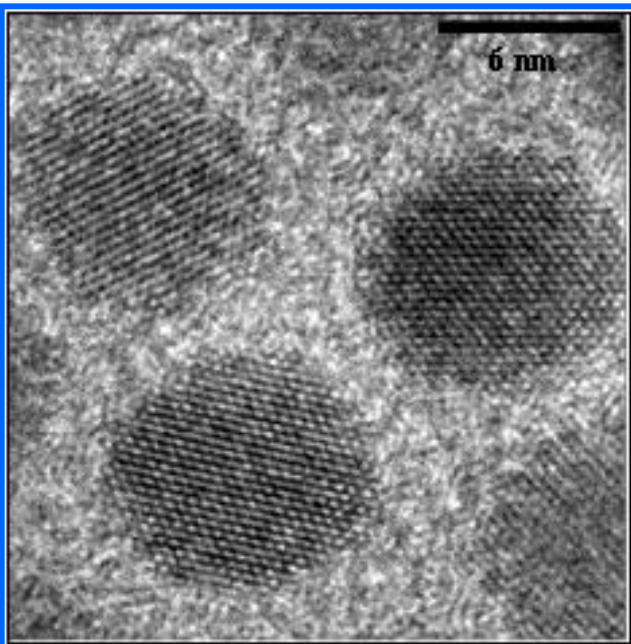


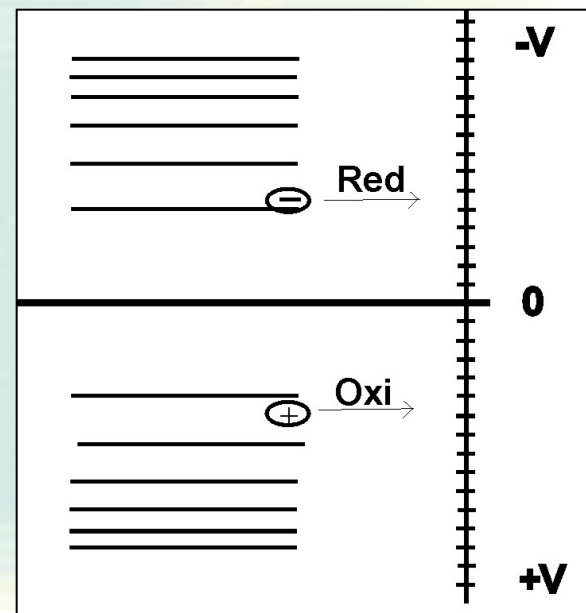
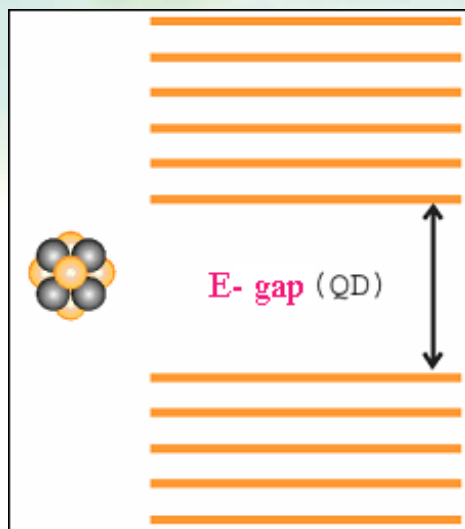
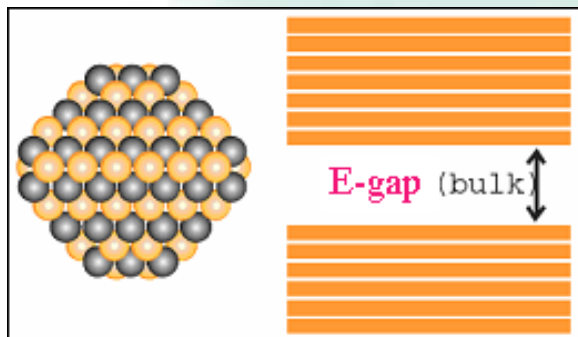
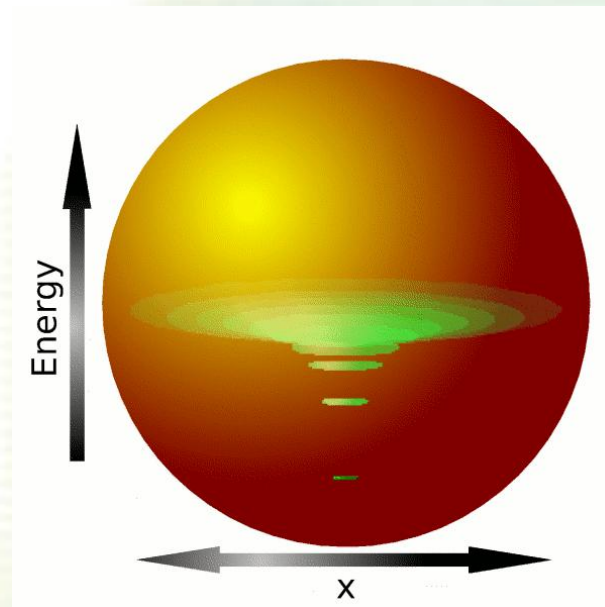
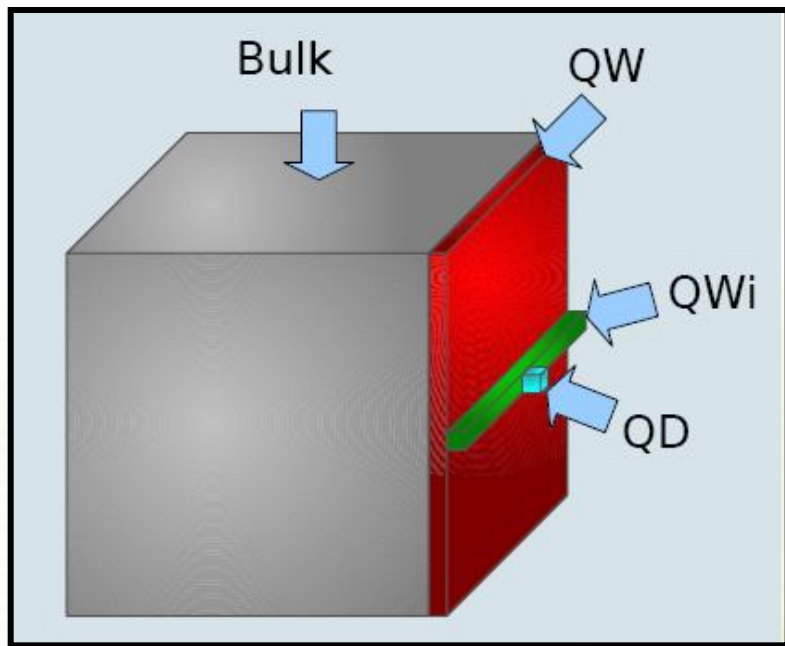
Selected Nanostructures produced by wet chemistry method



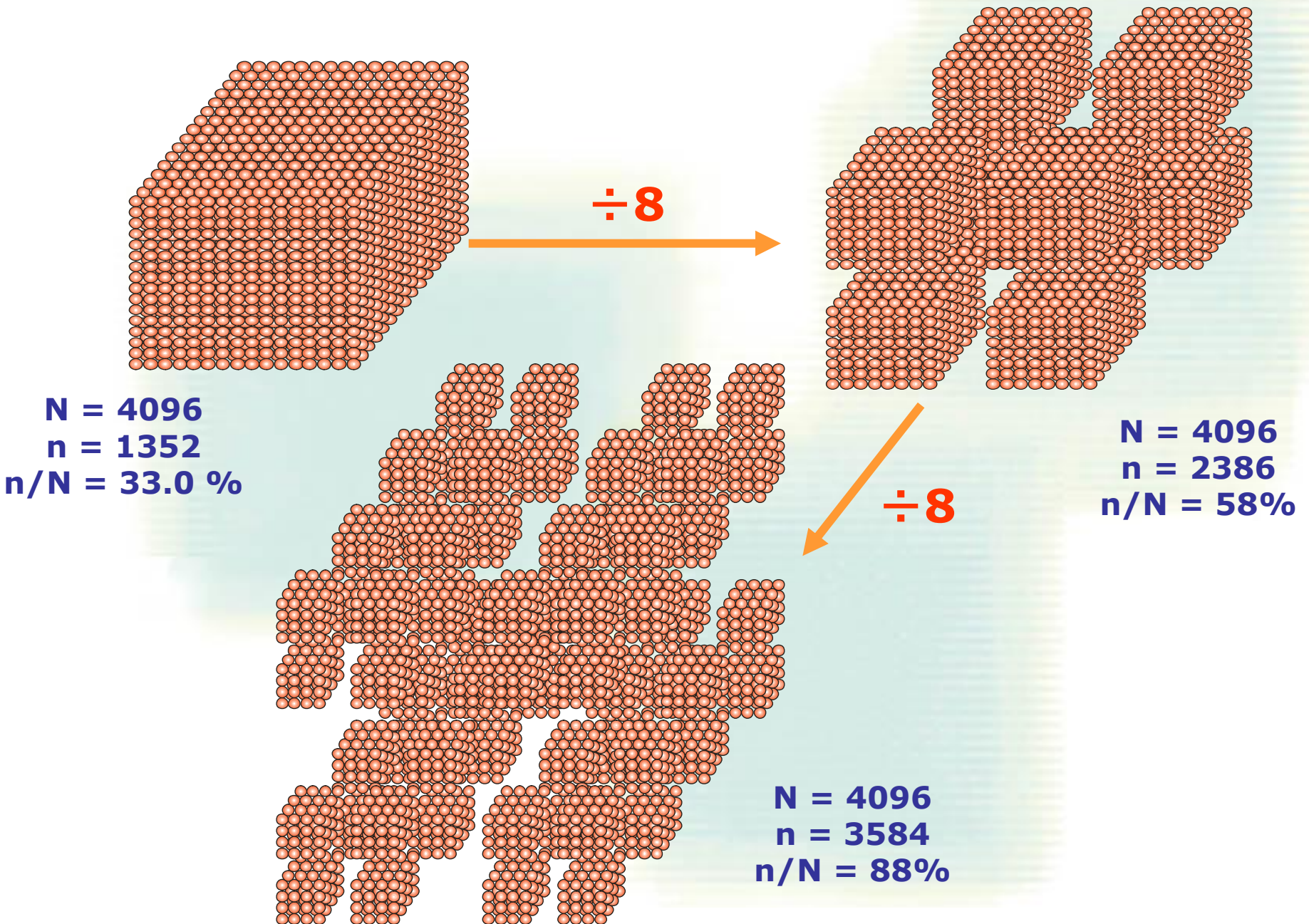
Particle / Q-dots /Bimetallic/ core –shell

Metallic and semiconductors Wires

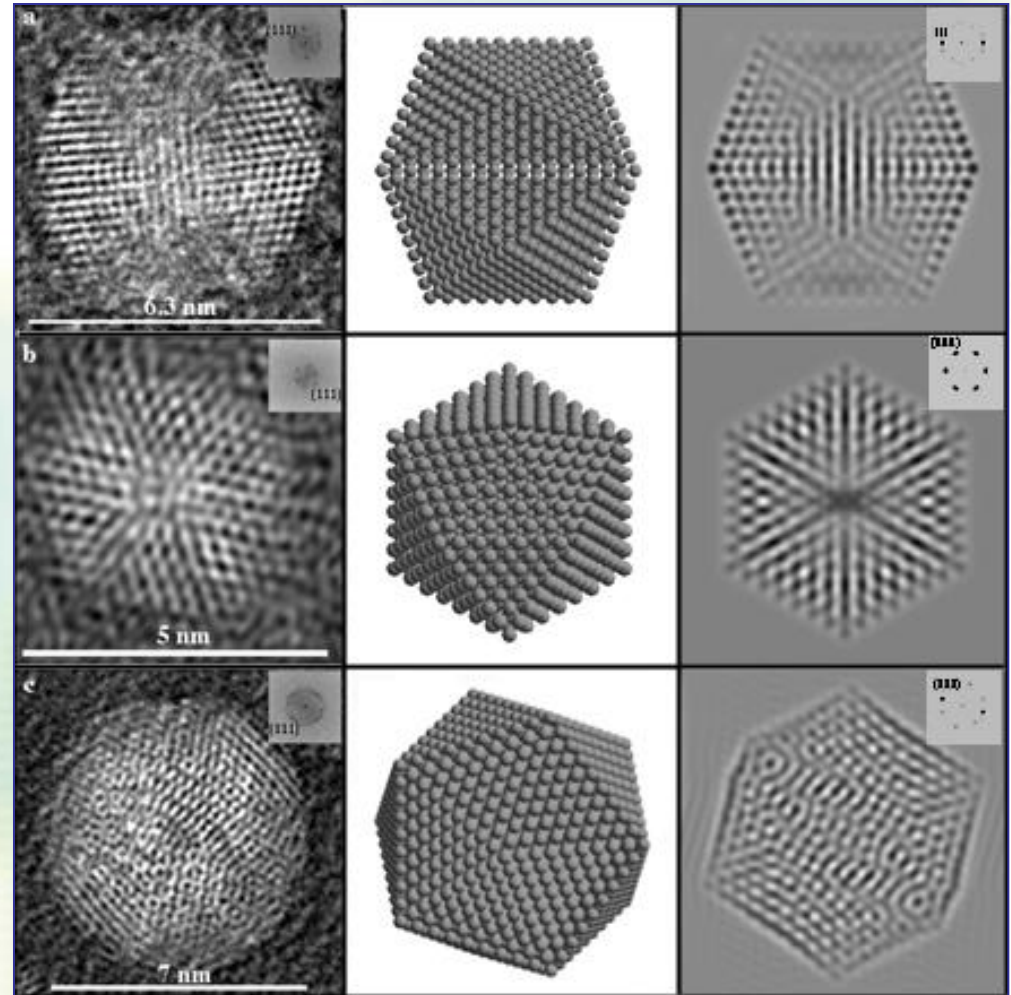
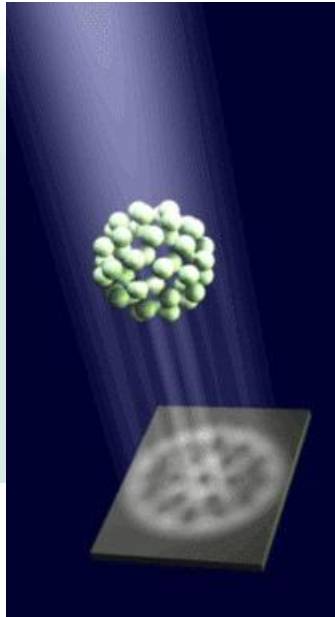
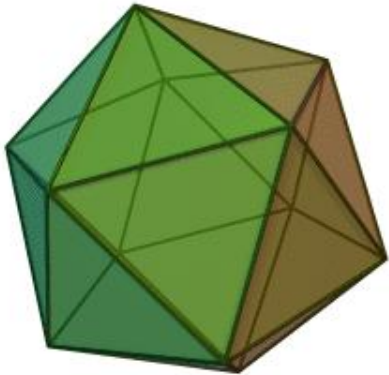
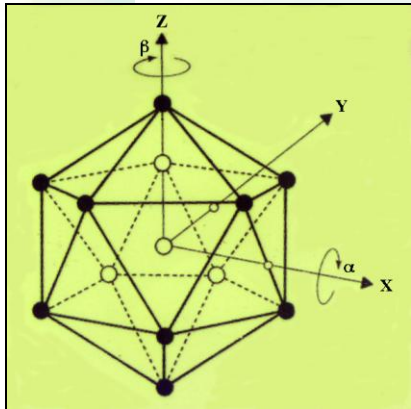




Surface: volume ratio



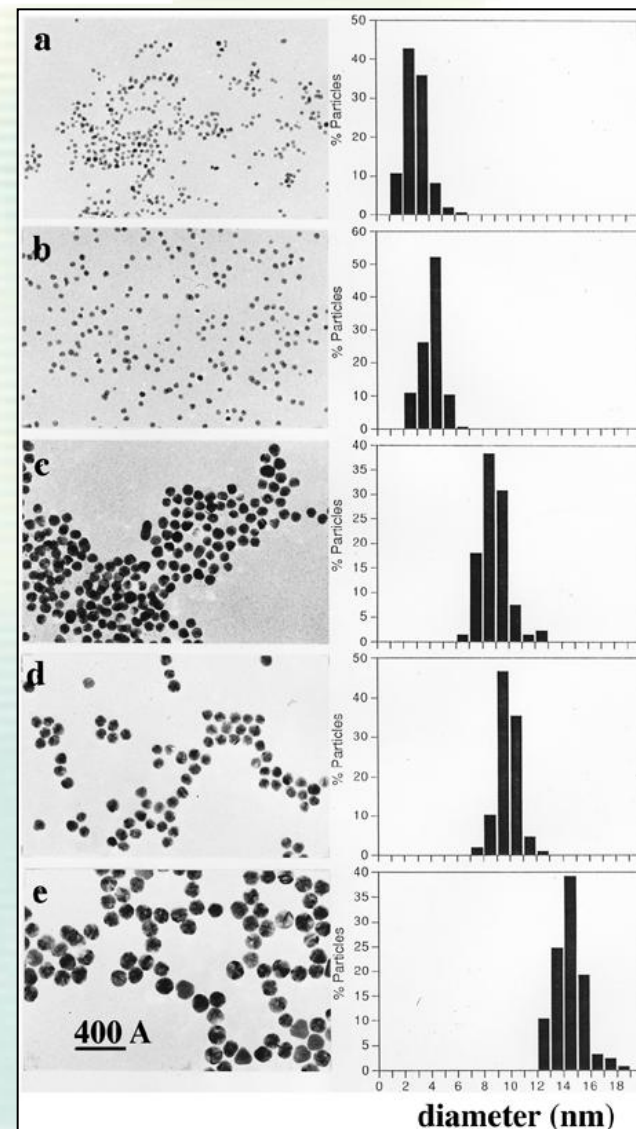
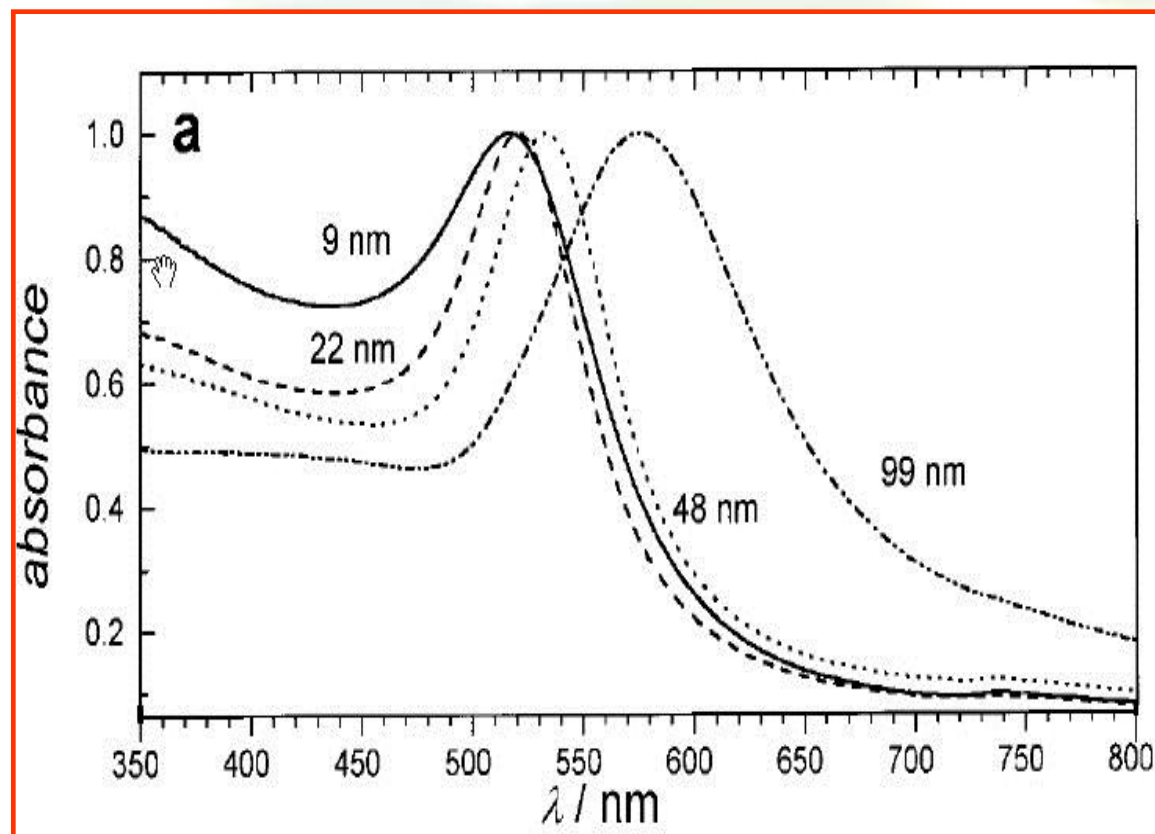
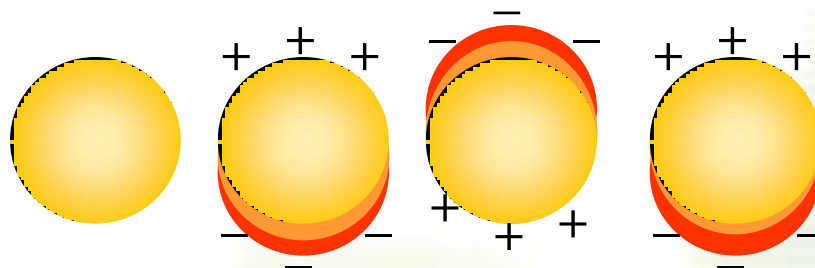
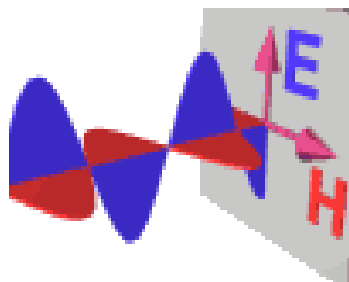
Experimental results and theory



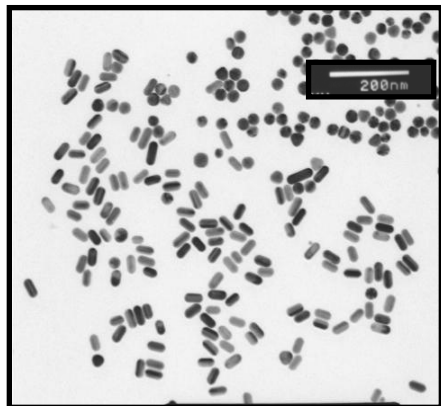
Giersig, M., et al., J. Phys. Chem., B 103, 9533-9539, 1999

Metal: (Ag,Cu, Pt..) **Au**-particles

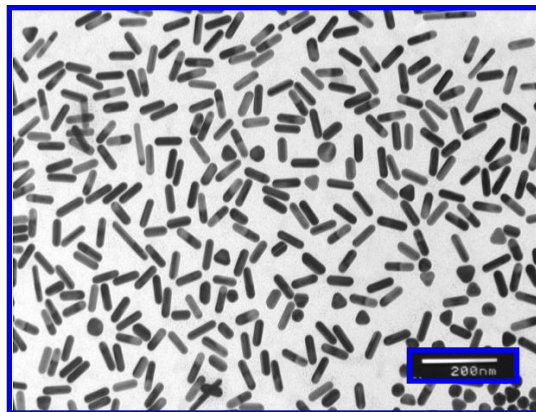
$$\omega_p = \sqrt{\frac{4\pi n e^2}{m}}$$



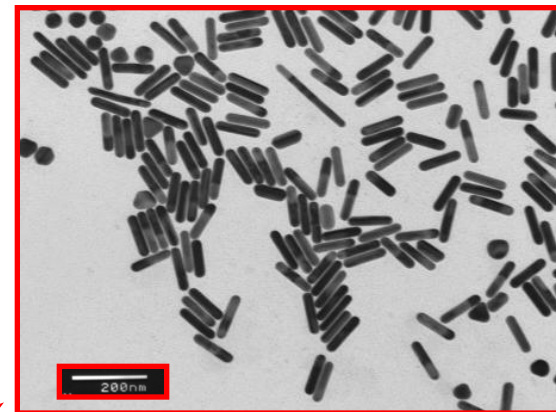
Different Aspect Ratios - Different Colours



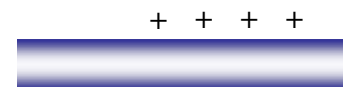
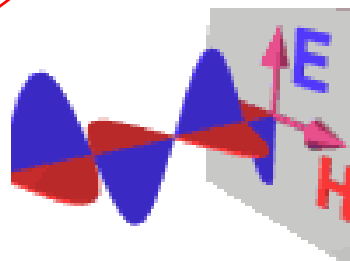
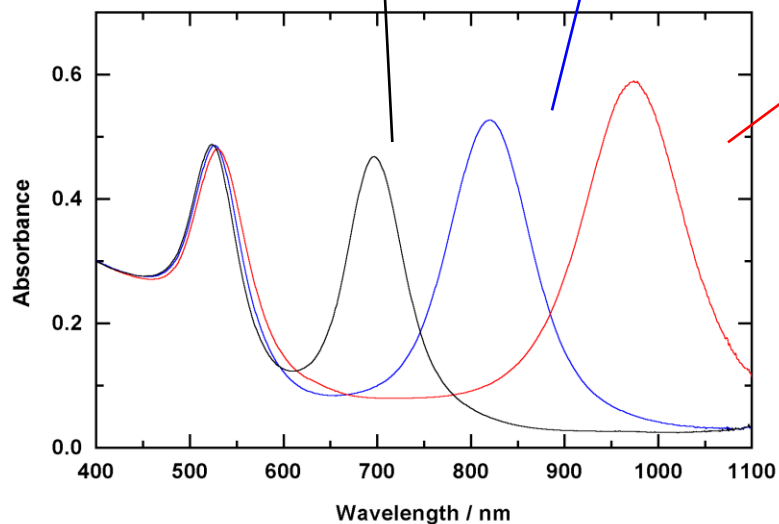
A.R.: 2.25
Width: 20.7 nm
Length: 46 nm



A.R.: 3.35
Width: 22.4 nm
Length: 75 nm



A.R.: 4.75
Width: 22.8 nm
Length: 108 nm

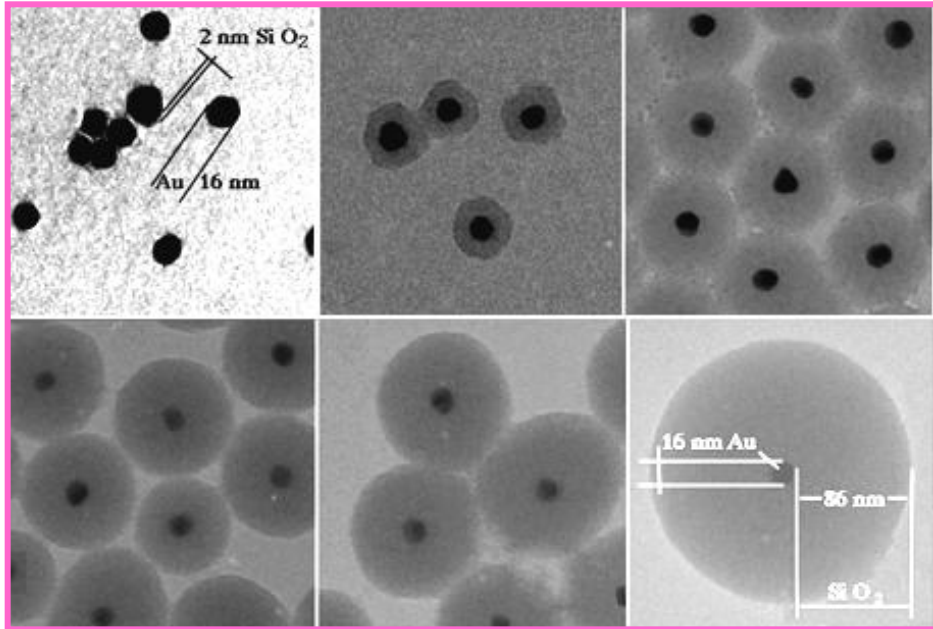


$$\omega_p = \sqrt{\frac{4\pi n e^2}{m}}$$



Pérez-Juste et al. Adv. Funct. Mat. 14, 571-579 2004
 Pérez-Juste et al. Chem Soc Rev 37, 1783-91 2008
 Pérez-Juste et al. Coord Chem Rev 249, 1870 2005

Successive growing process of SiO₂ on Au particles and their optical properties



Liz-Marzan L., Giersig M., Mulvaney P.,

LANGMUIR 12 4329-4335 1996

Giersig M., Ung T., Liz-Marzan L., and Mulvaney P.,

Advanced Materials 9, 570-575, 1997

1 - is a sputter coated gold 10nm

2 - 15 nm diameter Au-core particles + sodium citrate (0.5 nm)

3 - 15 nm diameter Au-core particles + sodium mercaptopropionate (1.0 nm)

4 - 15 nm diameter Au-core +

5 - 5 nm diameter Au-core +

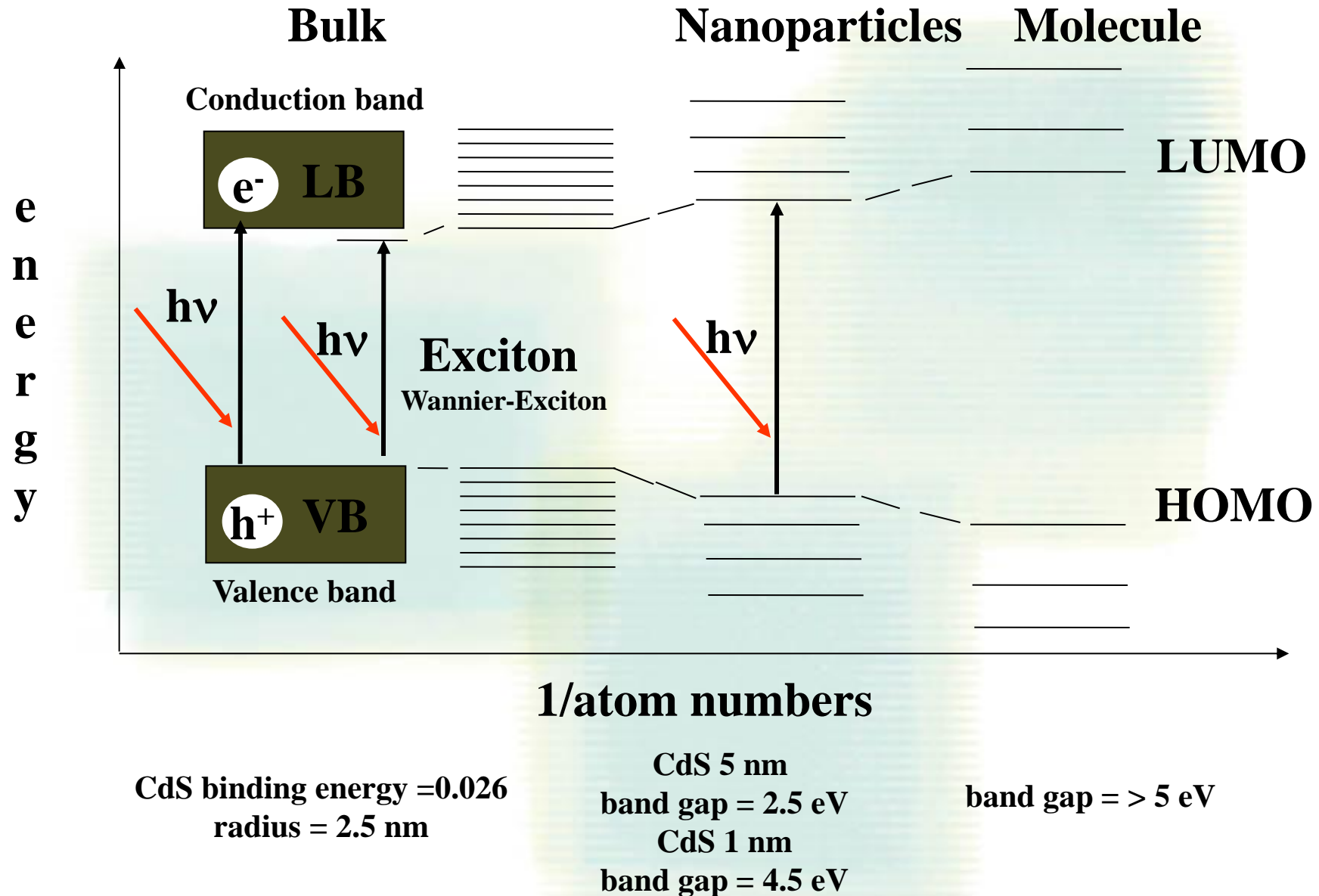
6 - 5 nm diameter Au-core +

7 - 5 nm diameter Au-core +

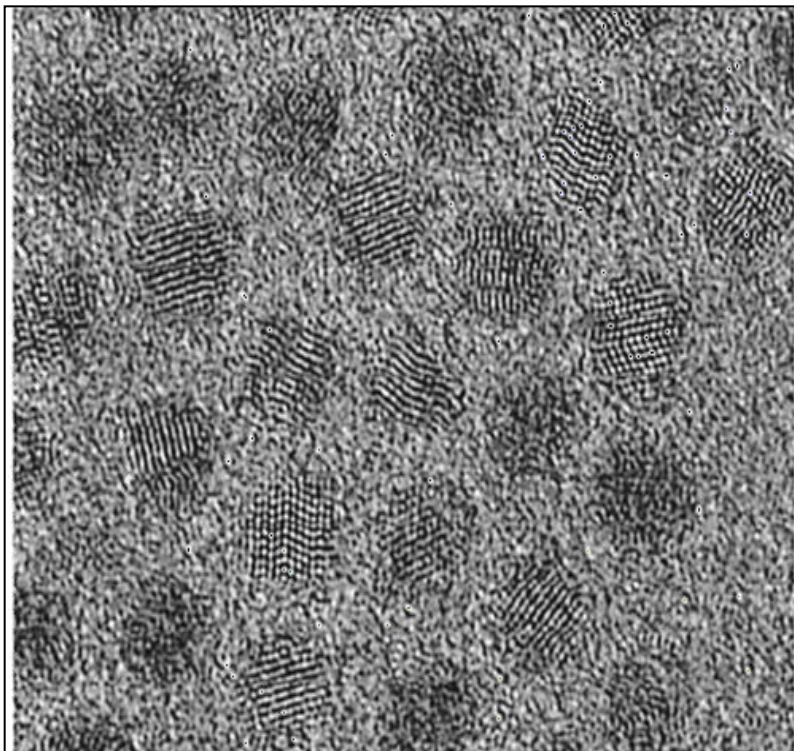
8 - 5 nm diameter Au-core +

Mulvaney P., Liz-Marzan L. M., Giersig M., and Ung T.,
J. Mater. Chem. 10, 1259±1270 2000

The electronic nature of the colloidal semiconductors



The nature of the colloidal semiconductors of different size



HRTEM CdSe/ZnS



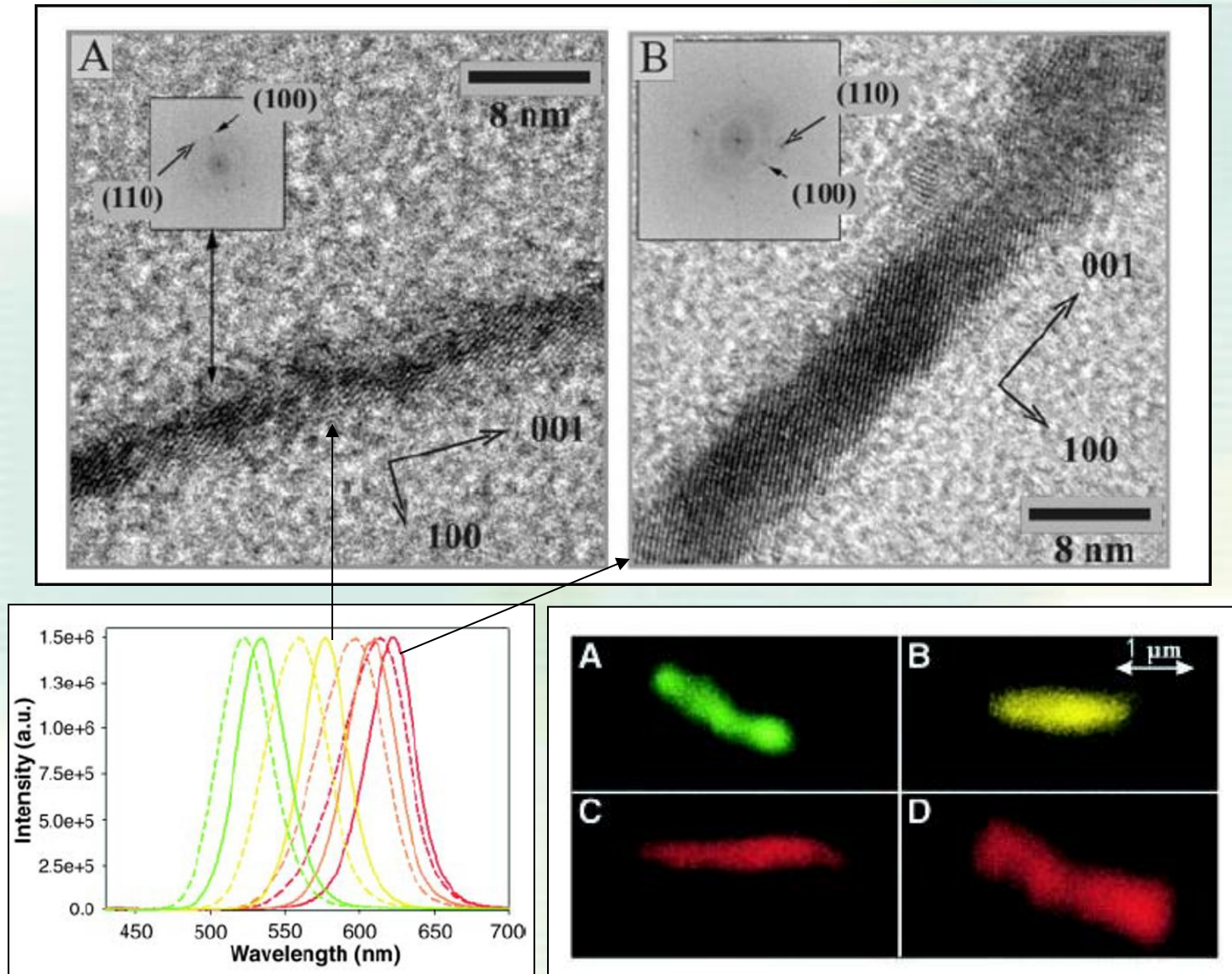
Water stable, biocompatible CdSe/ZnS nanoparticles of different size (1,8--3,1 nm)

van Embden, J., Jasieniak, J., Gomez, E., et al.

Review of the synthetic chemistry involved in the production of core/shell semiconductor nanocrystals

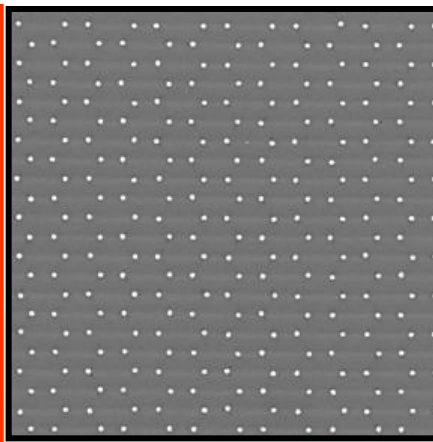
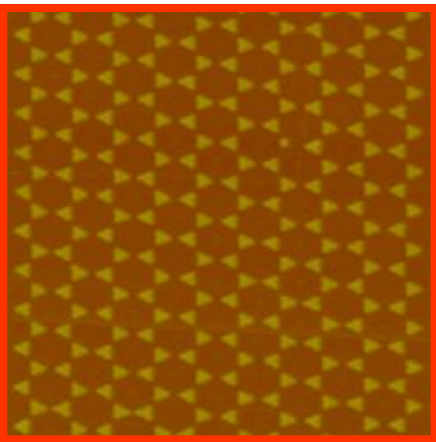
AUSTRALIAN JOURNAL OF CHEMISTRY 60 7 457-471 2007

CdTe nanowires

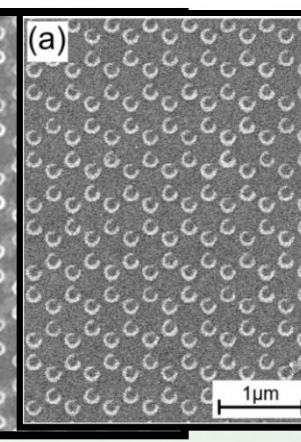
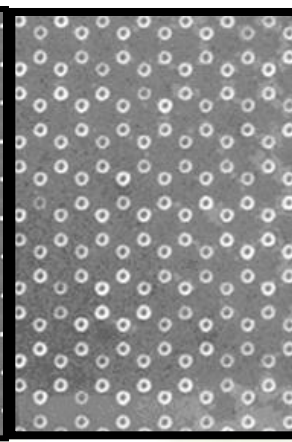


Selected Nanostructures produced by physical method

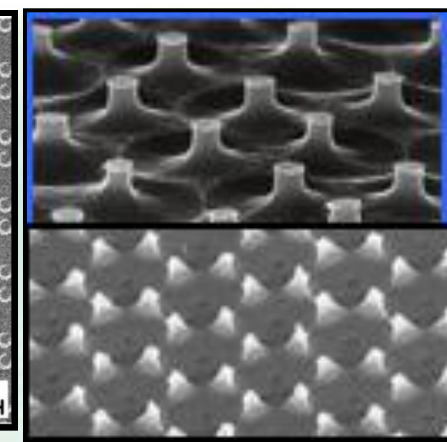
Triangles spherical shape



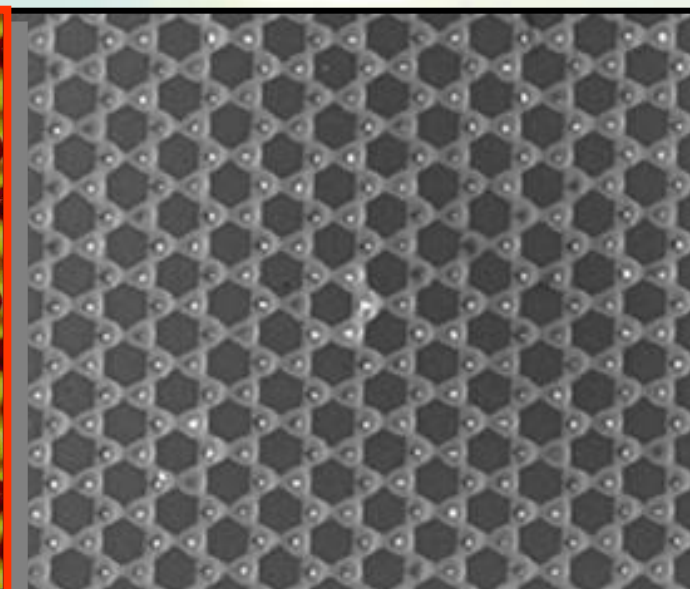
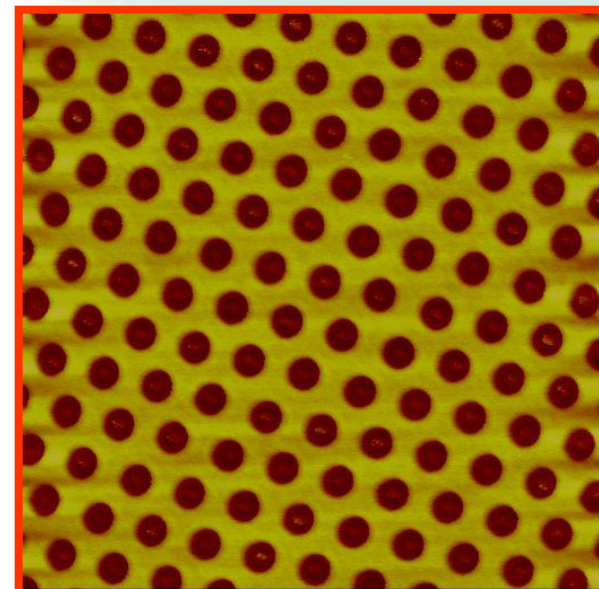
Nanorings



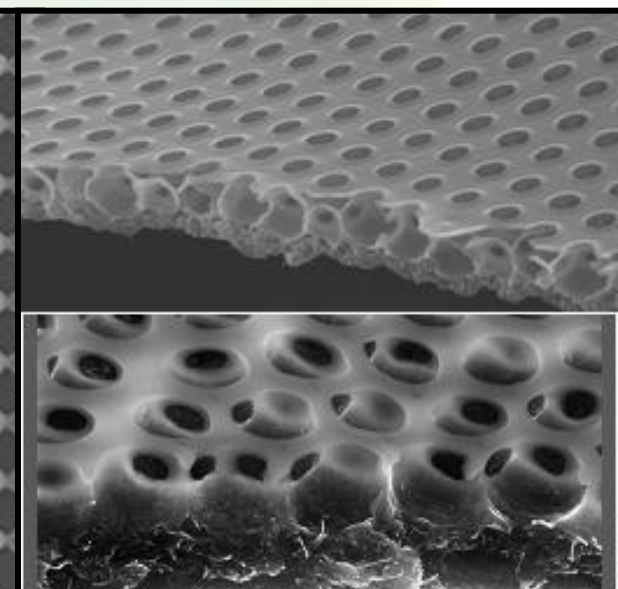
Pillars/Pyramids



Nanoholes

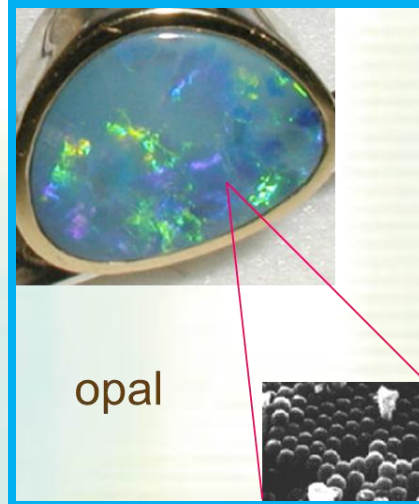
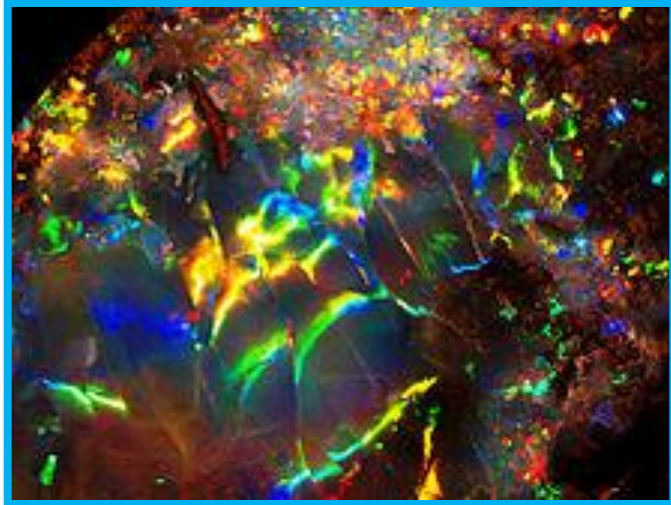


Bimetallic

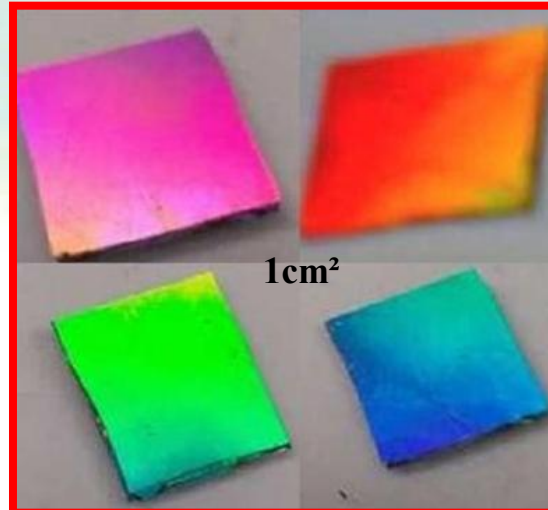
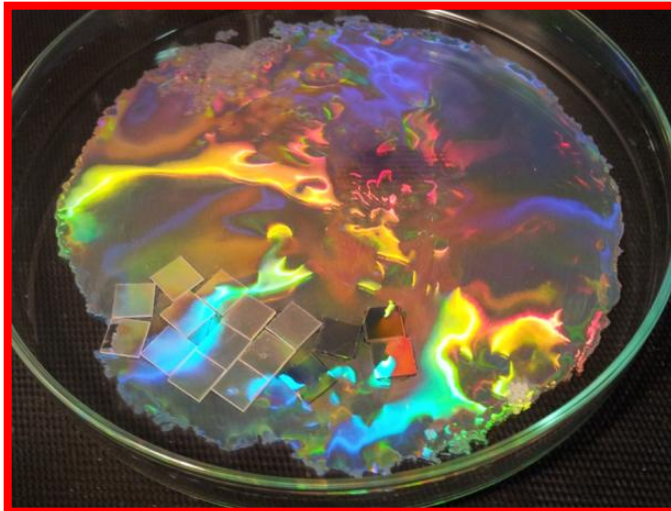


3-D Structures

Examples of natural and artificial made Opals

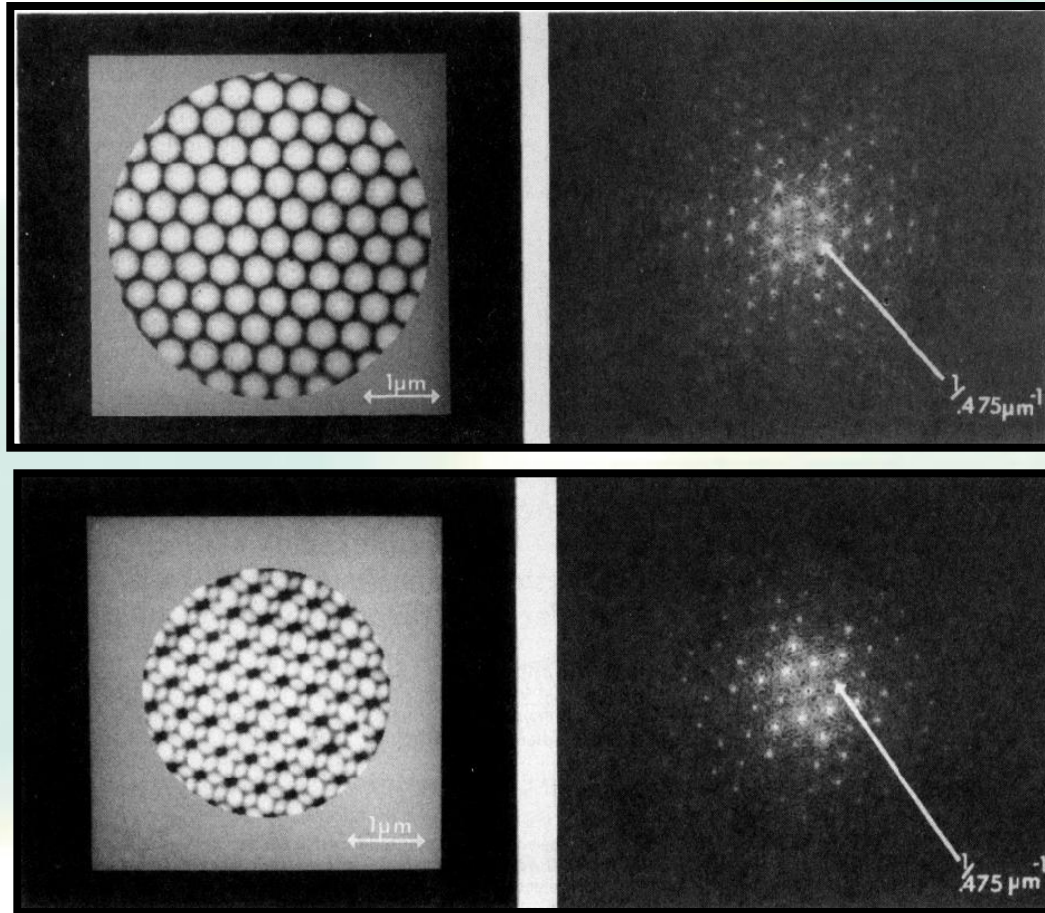


An opal bracelet.
The stone size is 18 by 15 mm.
Opal is composed of silica spheres
some 150 to 300 nm in diameter in
a hexagonal or cubic close-packed lattice



Photographs of 2-D a hexagonal
close-packed lattice based on
490 nm in diameter Latex particles

2D ordered latex monolayer prepared by electrophoresis

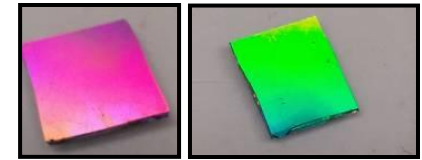
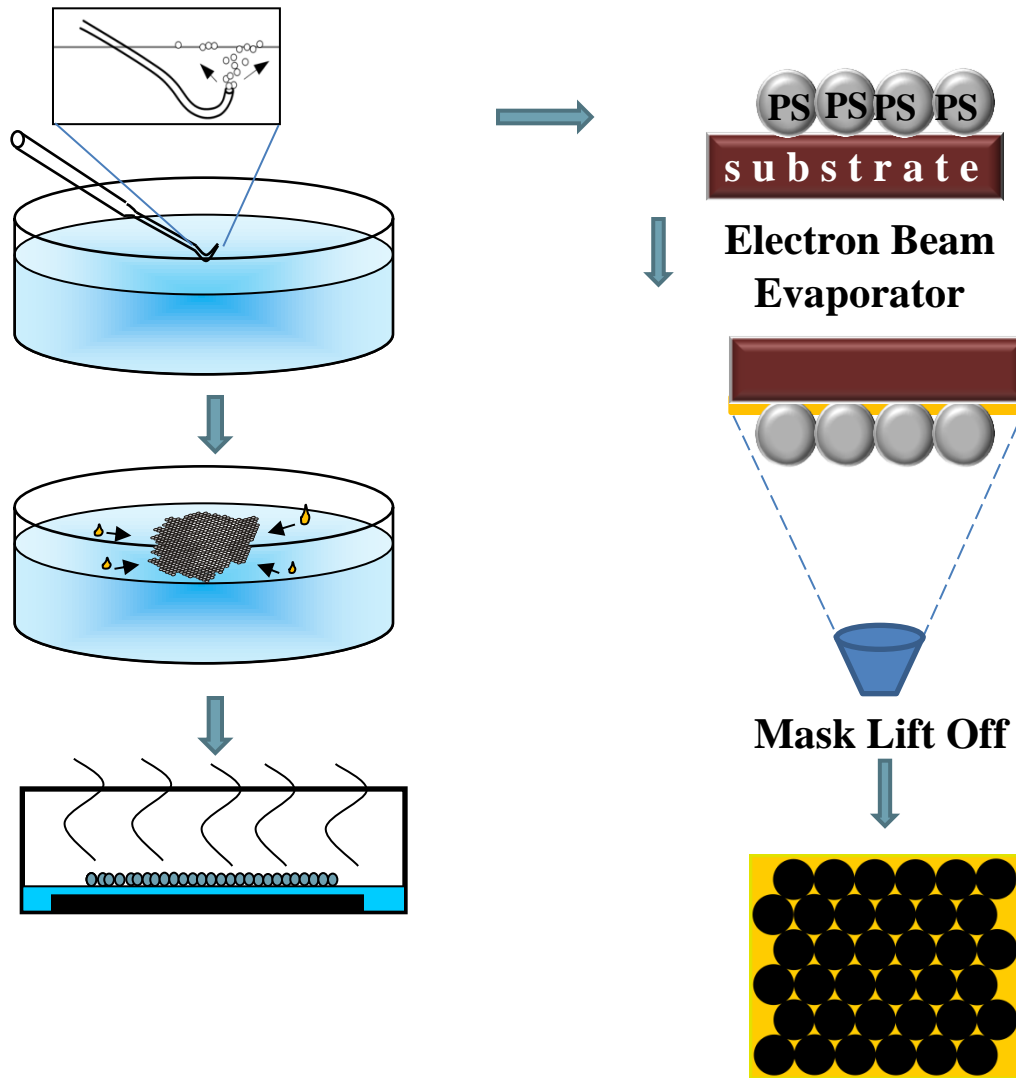


In the left row TEM images of the 2-D and 3-D structures based on Latex particles with the mean particle size of 440 nm and their Fourier transform respectively, showing numerous higher order reflexes (right).

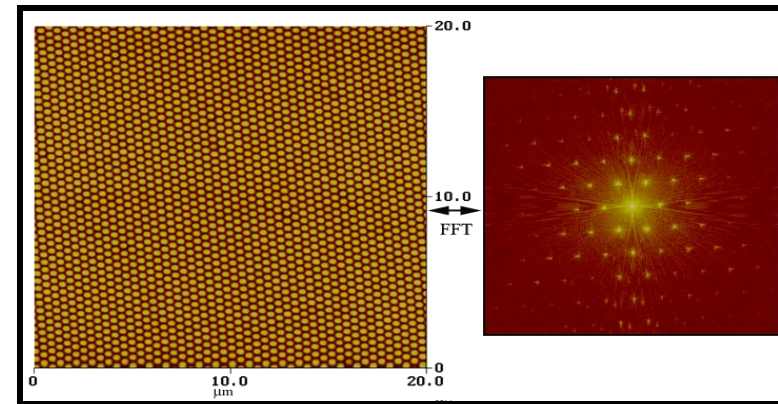
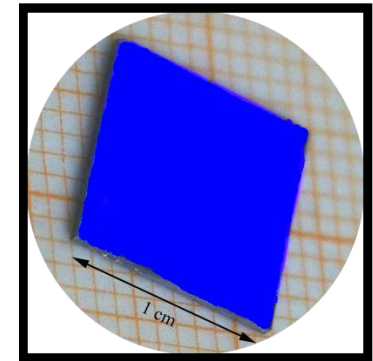
Giersig M. and Mulvaney P.

Preparation of Ordered Colloid Monolayers by Electrophoretic Deposition; *Langmuir* 9, 3408-3413, 1993

General introduction to NSL



hcp masks on Si substrates



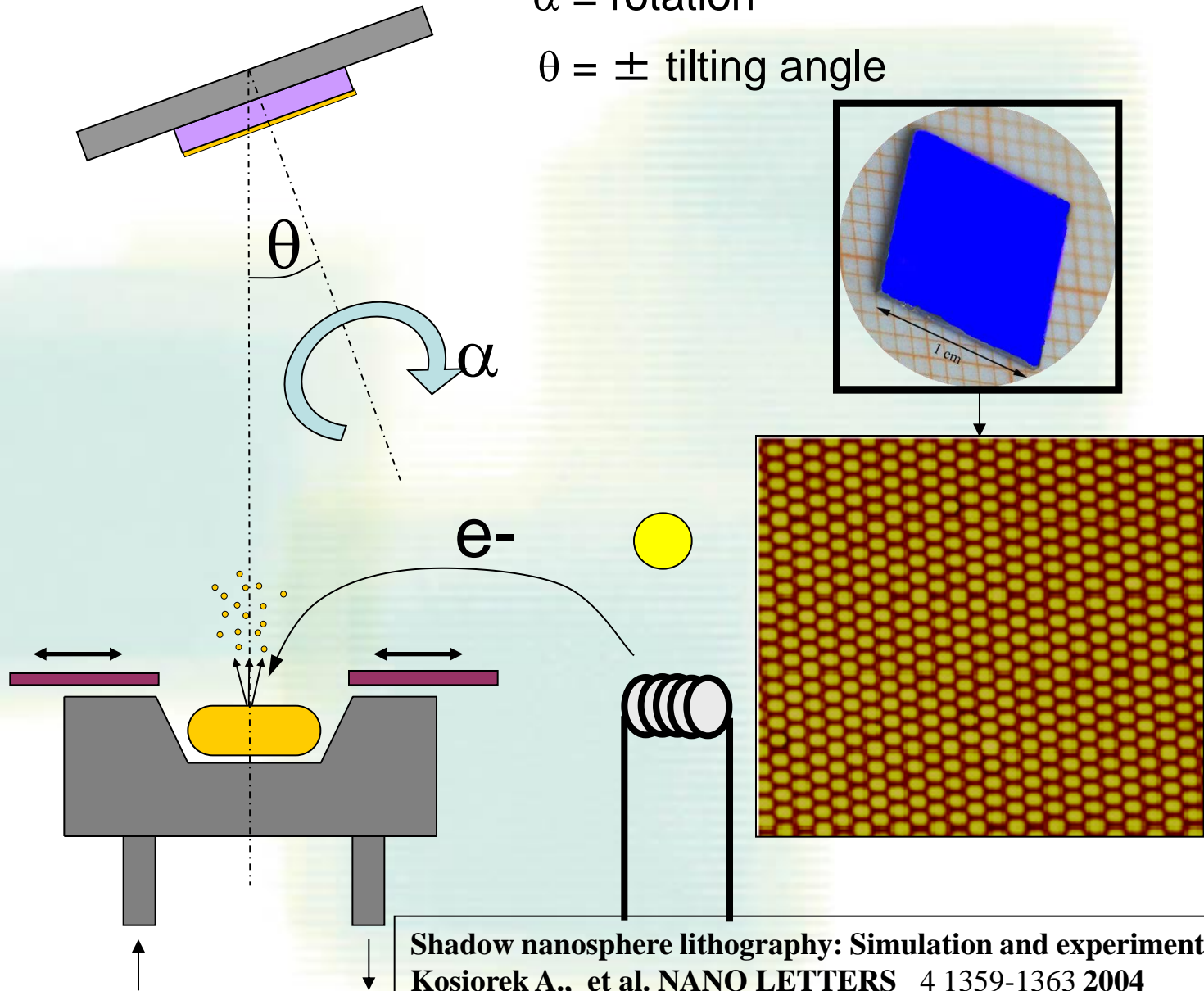
Rybczynski J., Ebels U., Giersig M.,

Large-scale, 2D arrays of magnetic nanoparticles; COLLOIDS AND SURFACES A 219 1-3 1-6 2003

Geometry of an electron beam evaporation system

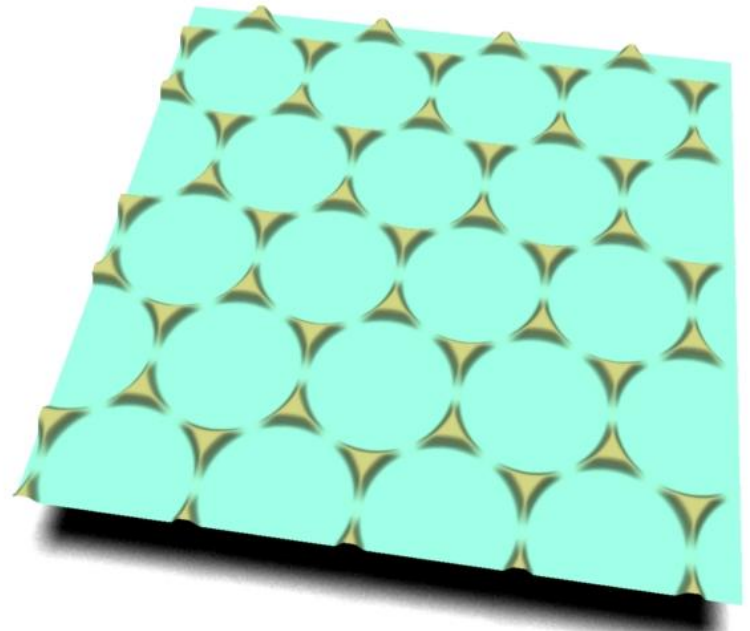
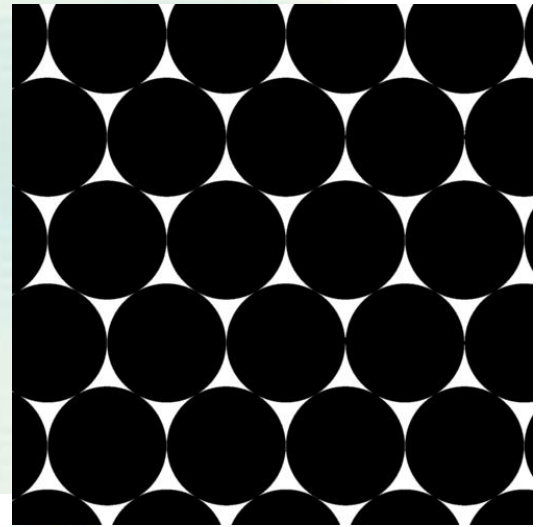
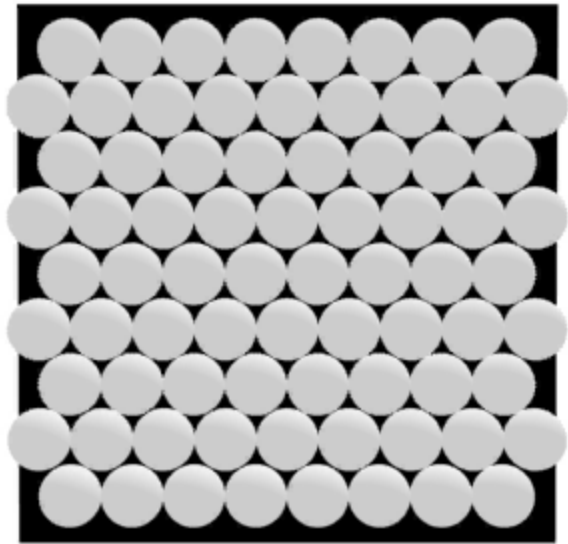
α = rotation

$\theta = \pm$ tilting angle

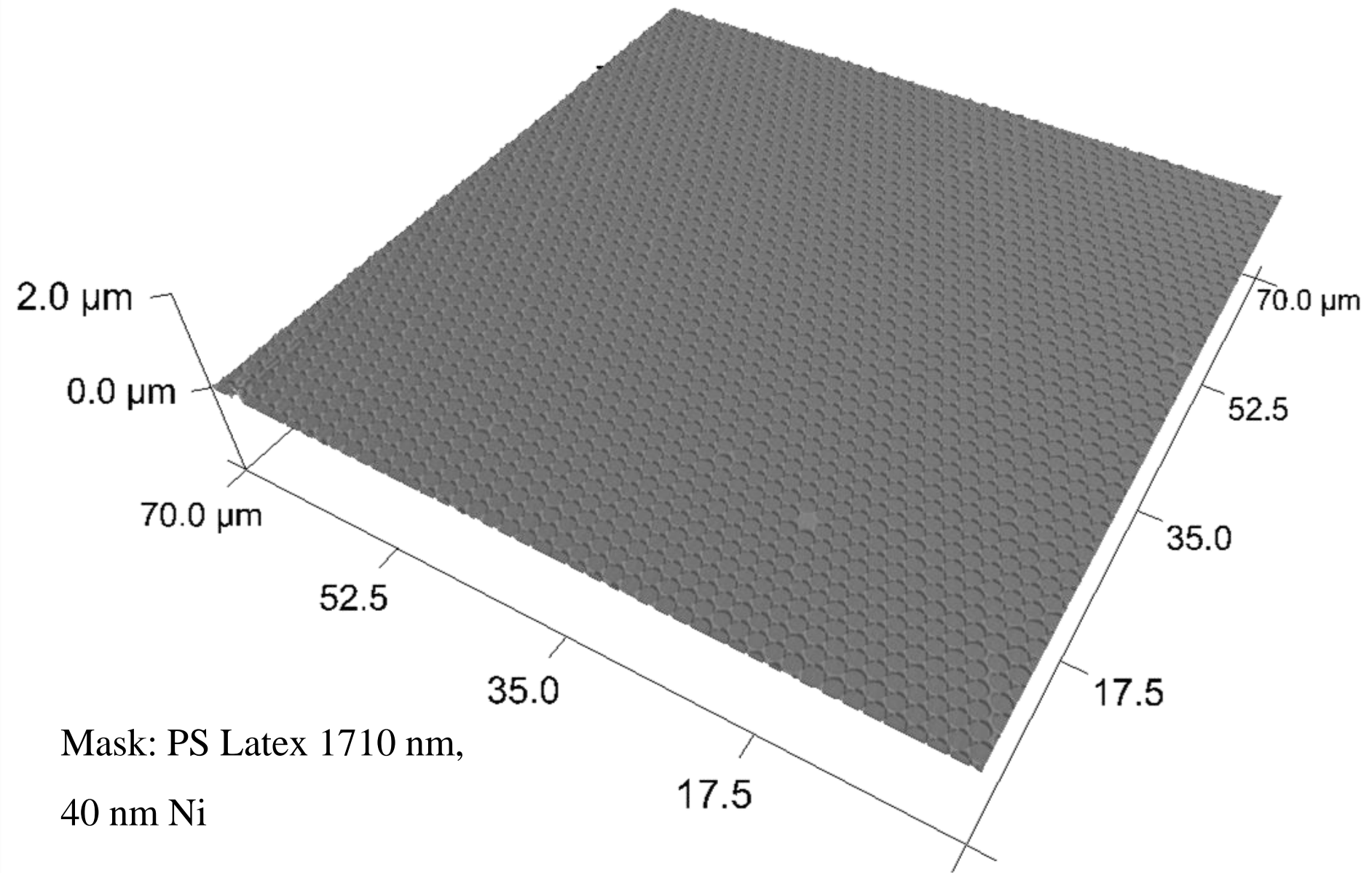


Simulation

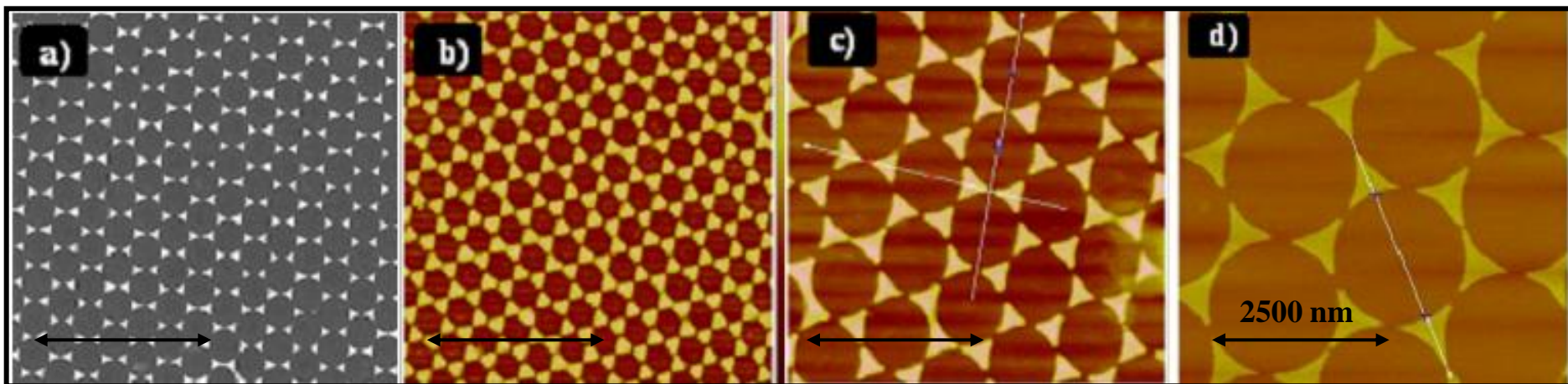
evaporation angle 90°



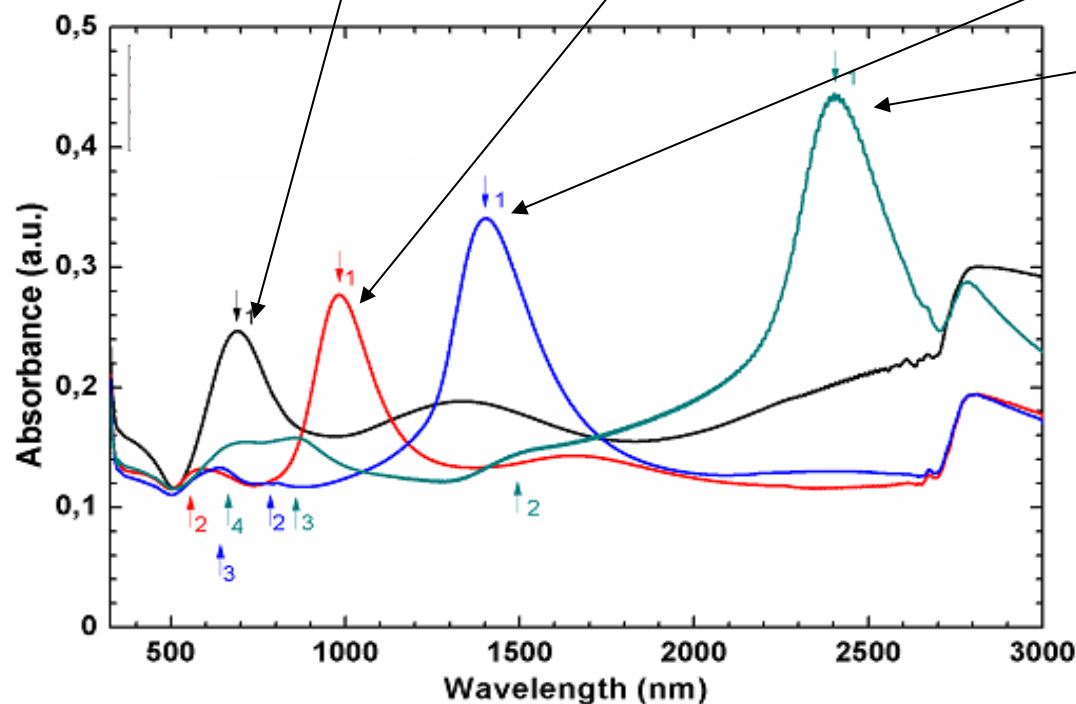
Large 2-D nanotriangles structures



Plasmonic properties of array of triangular shaped gold nanoislands



PS-diameter $a =$ 380 540 980 1710 nm



Important!!

The spectra exhibit first (most pronounced)
Second and third and fourth absorbance peaks

It is expected, that these resonances are from a
highly dispersive, plasmon
polaritonic mode since similar resonances have
been observed in metallic particles


The experimental spectra for 20 nm thick Au triangles on a sapphire substrates

Theoretical approach

The experimental spectra shown for structures obtained with sphere diameters $a = 380, 540, 980, 1710$ nm,

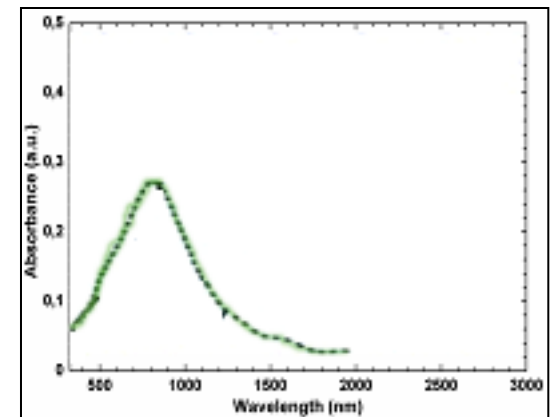
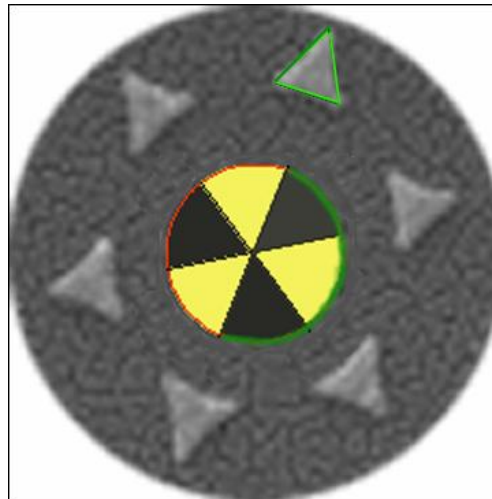
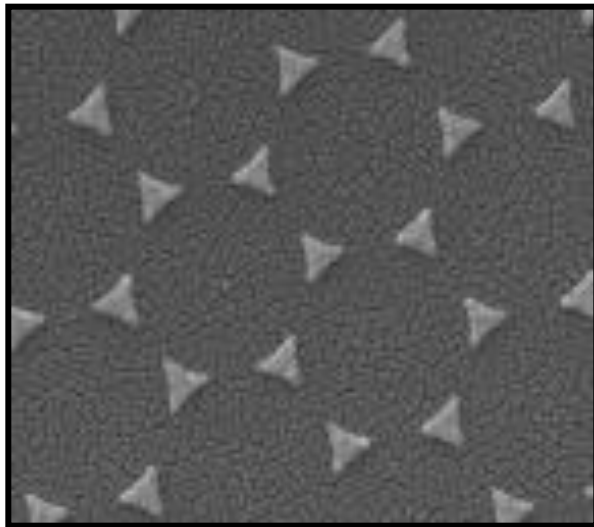
Each spectrum is dominated by a pronounced resonance peak, position of which strongly depends on a .

We assume, that these resonances can be viewed as circumferentially quantized surface plasmon waves and ignore the particle-particle interactions.

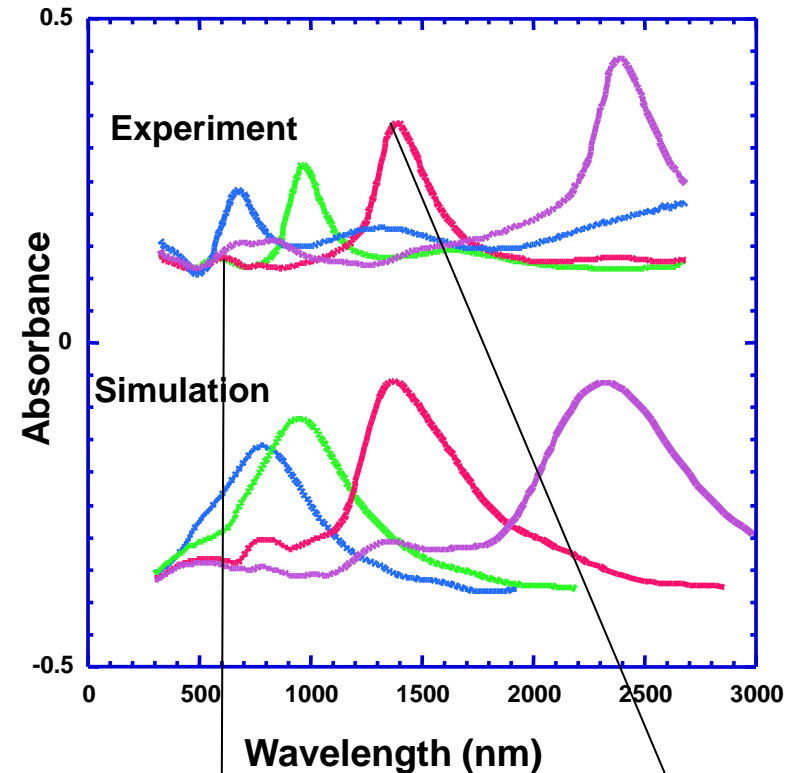
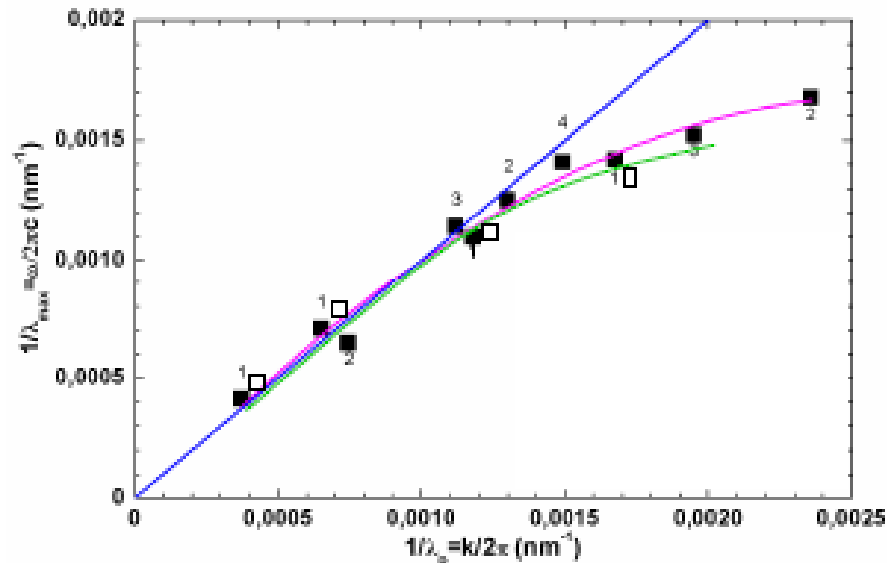
Since each side of the quasi-triangular  particle equals approximately 1/6 of the sphere circumference πa

The circumference of the particle $\sim \pi a / 2$ and thus the circumference quantization condition requires that this circumference is equal an integral multiple (l) of the wavelengths of the resonating surface/edge plasmon wave (λ_p)

$$l \lambda_p \sim \pi a / 2$$



Surface plasmon resonances in metallic nanoparticles:



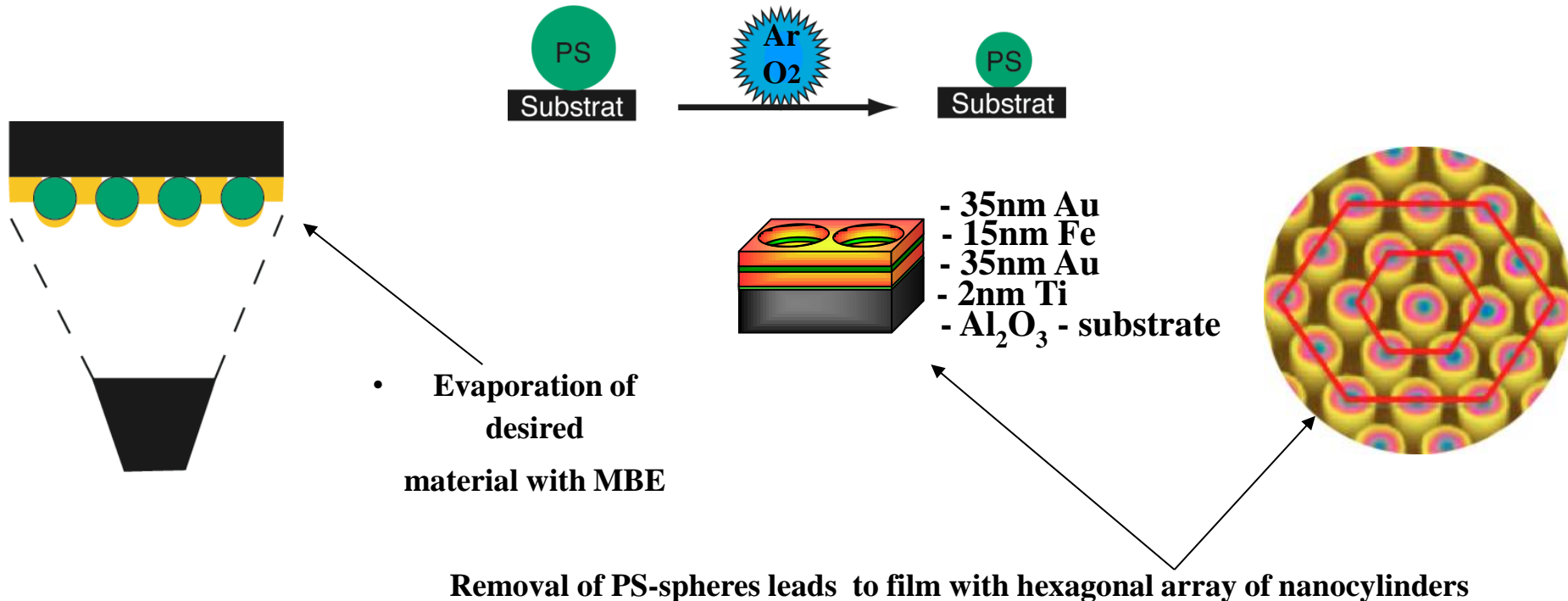
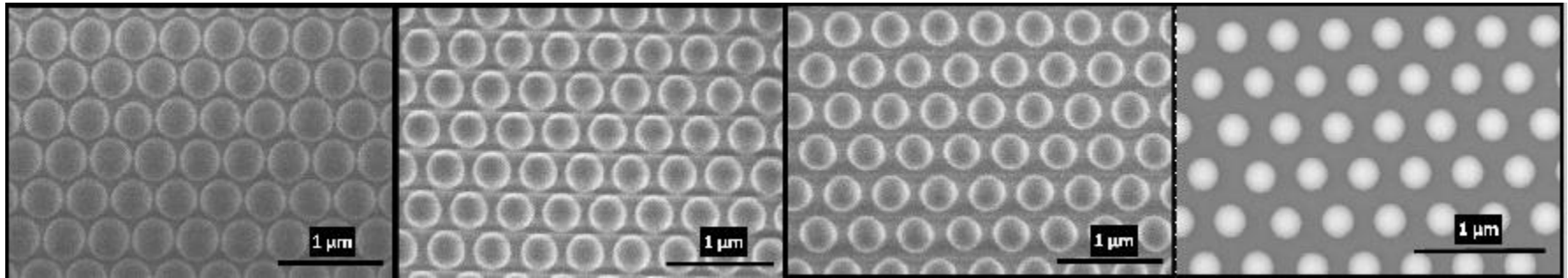
	D_0 [nm]							
	380		540		980		1710	
l	λ_{max}	λ_{sp}	λ_{max}	λ_{sp}	λ_{max}	λ_{sp}	λ_{max}	λ_{sp}
1	704	597	996	848	1417	1539	2417	2686
2	-	298	596	424	799	769	1551	1343
3	-	198	-	282	658	513	875	895
4	-	149	-	212	-	385	709	671



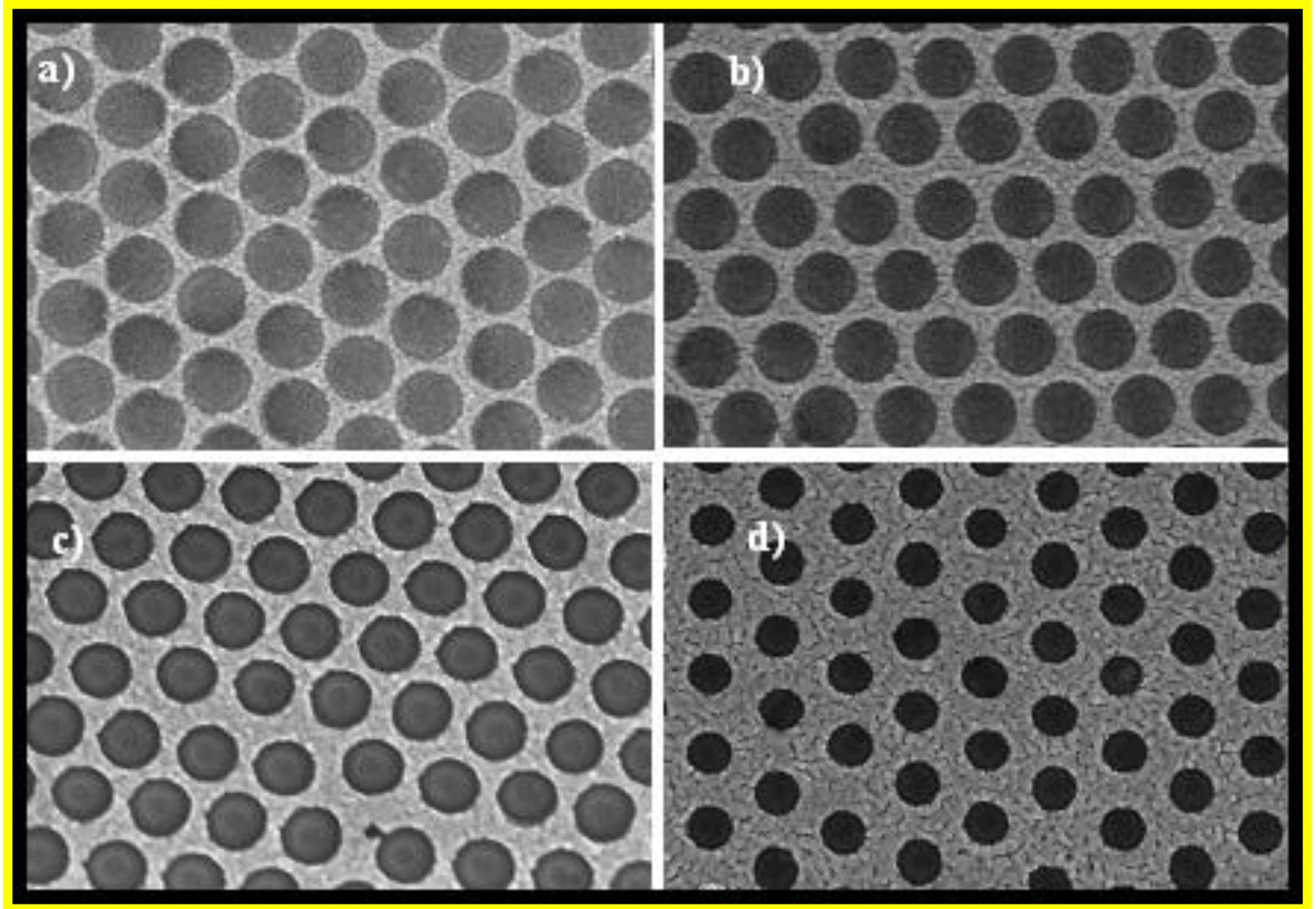
2-D nanocylinders :

Light Transmission and manipulation of dielectric constant

Mask modification - reactive ion etching (RIE) for reduction of PS-diameter

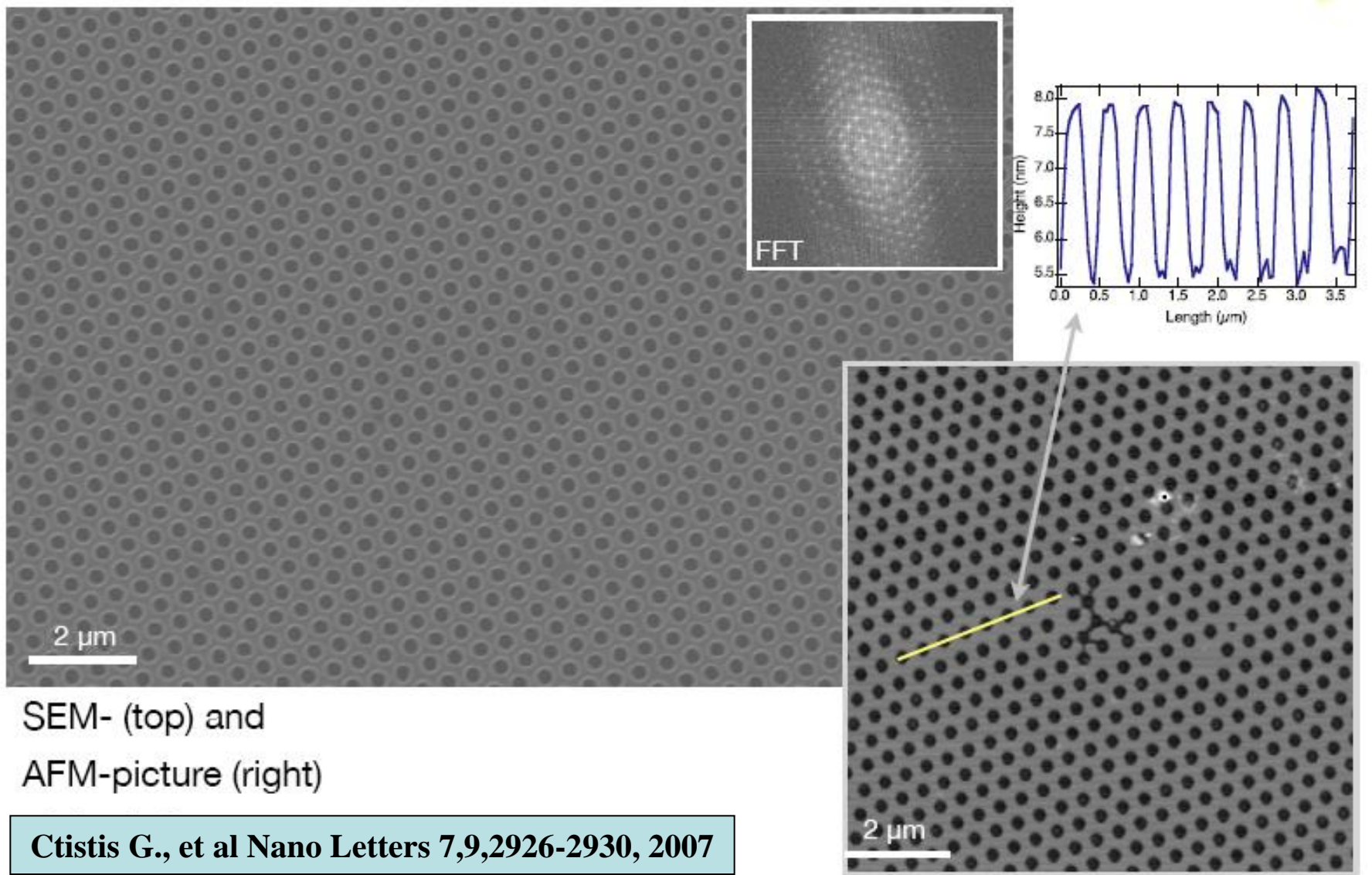


Example of 2-D arrays of nanocylinders



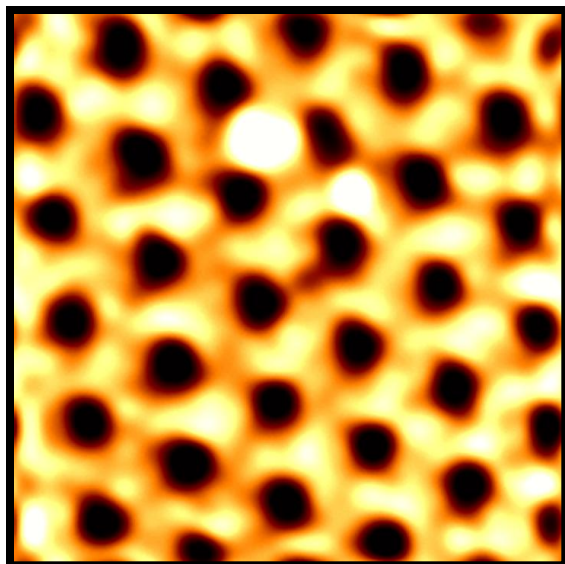
SEM images of nanocylinder arrays. Diameter of single hole is a) 385nm, b) 340nm, c) 325nm and d) 265nm

Characterization of 2-D structures

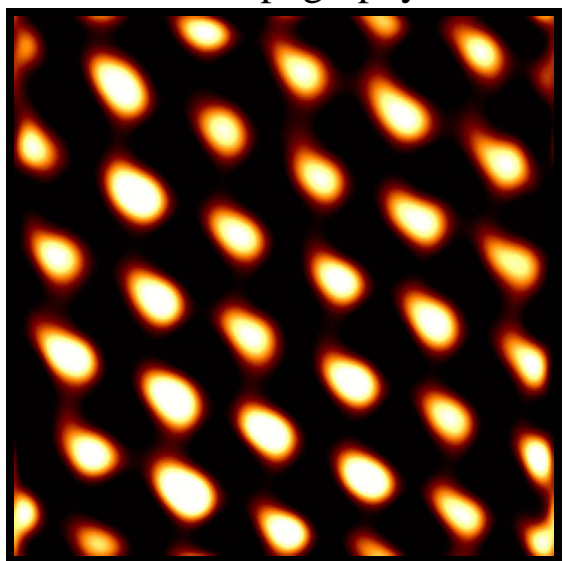


Nano-hole arrays / Plasmonic metal

SNOM pictures for a 50 nm thick gold film



topography



near-field optics

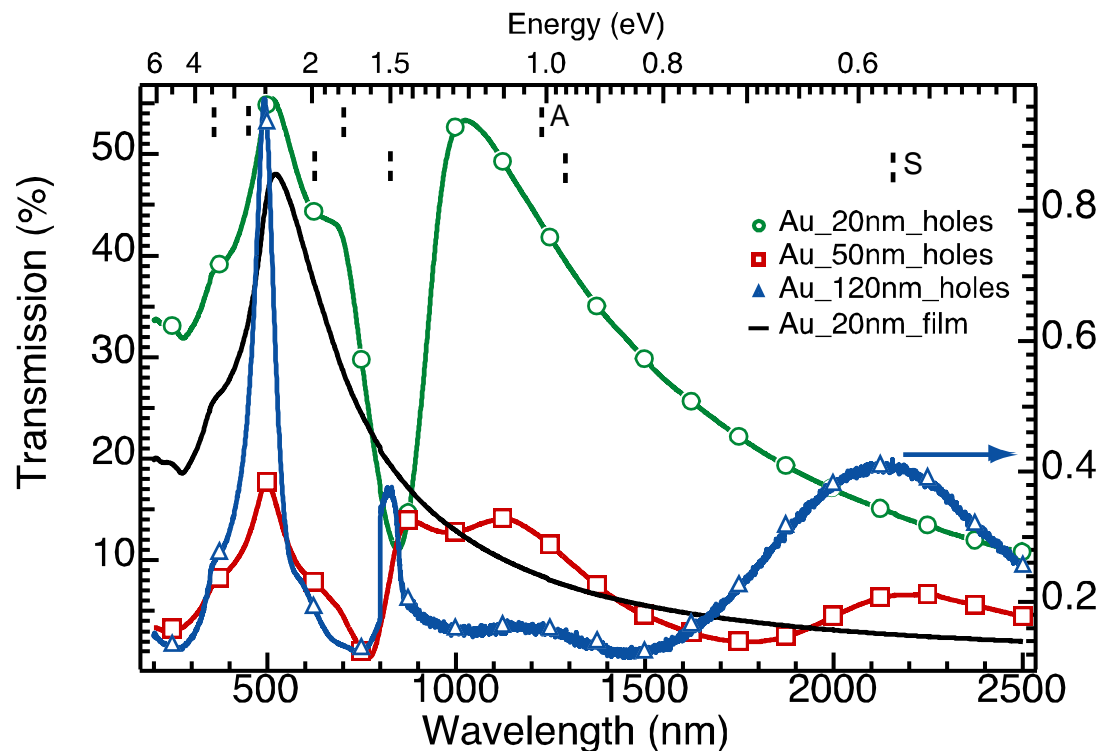
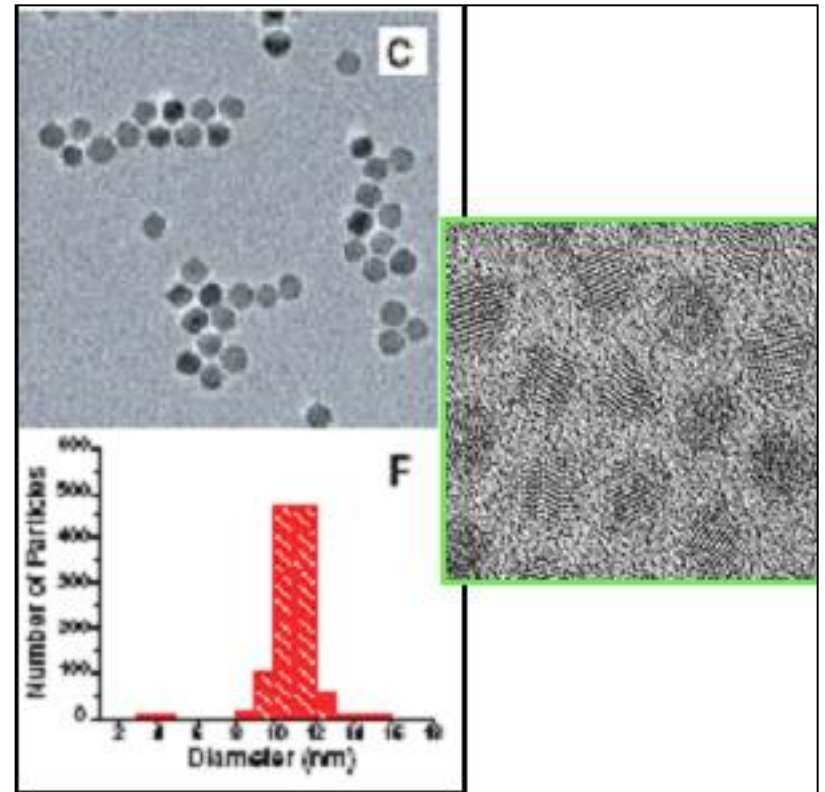
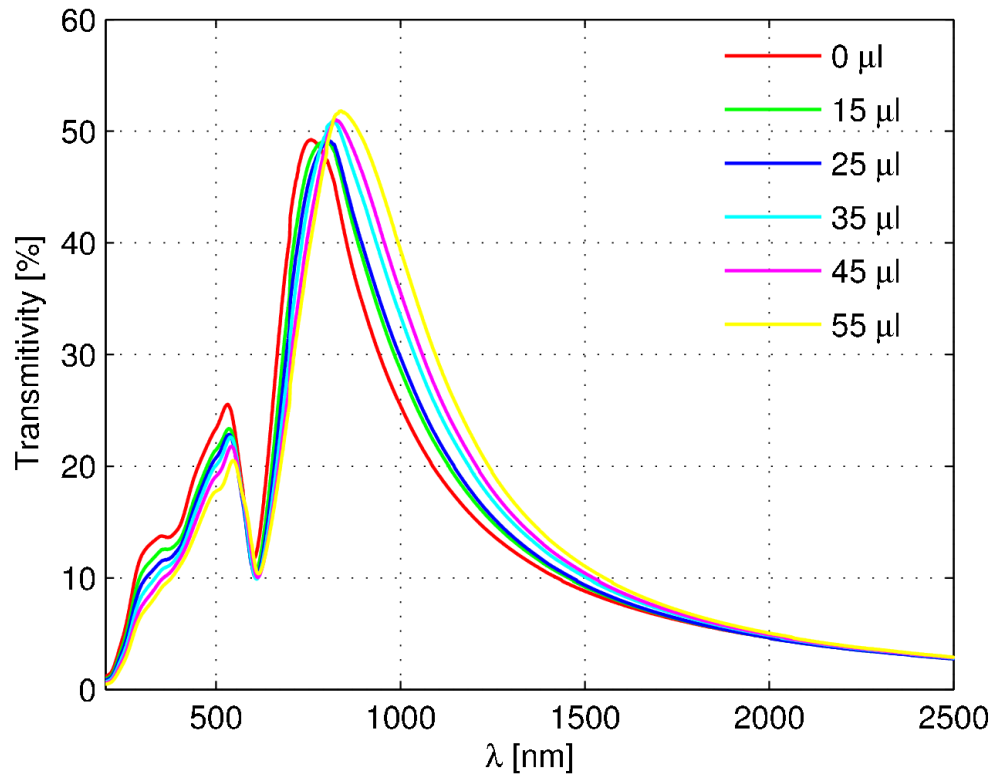


Image size: $(3.5 \mu\text{m})^2$

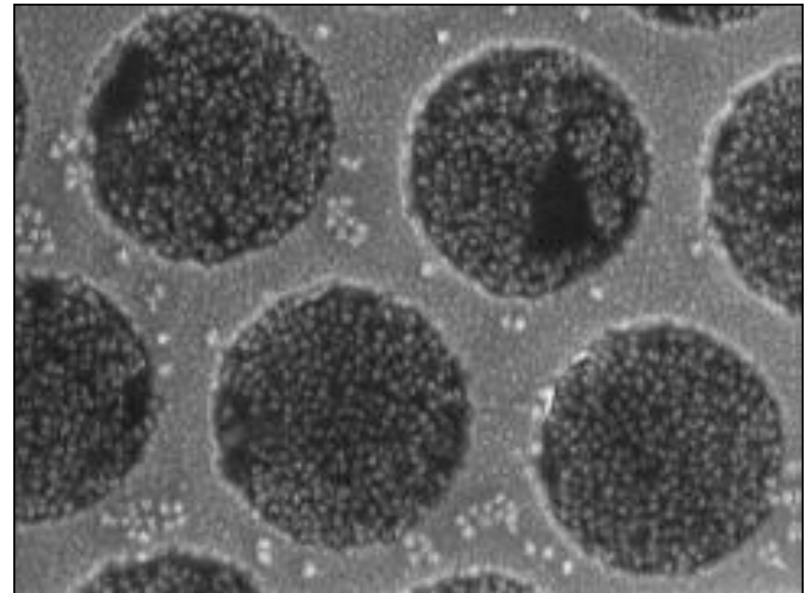
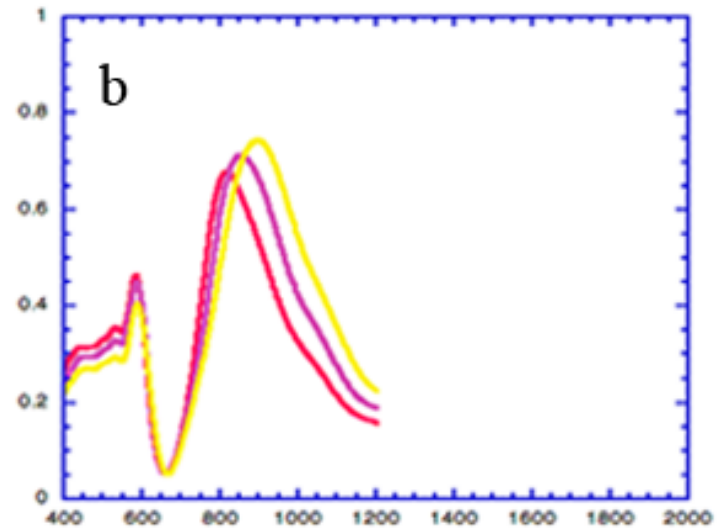
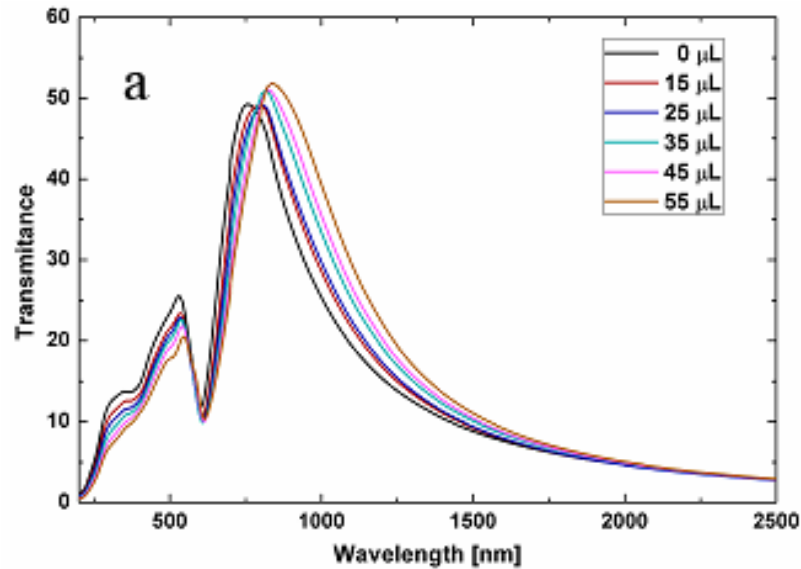
○ Main transmission path through the holes

Au/Fe/Au – influence of Fe_3O_4 particles

- subsequent addition of Fe_3O_4 nanoparticles on the sandwich structure introduced changes in the position and intensity of the transmission peaks

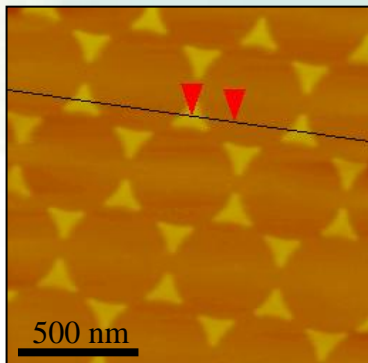
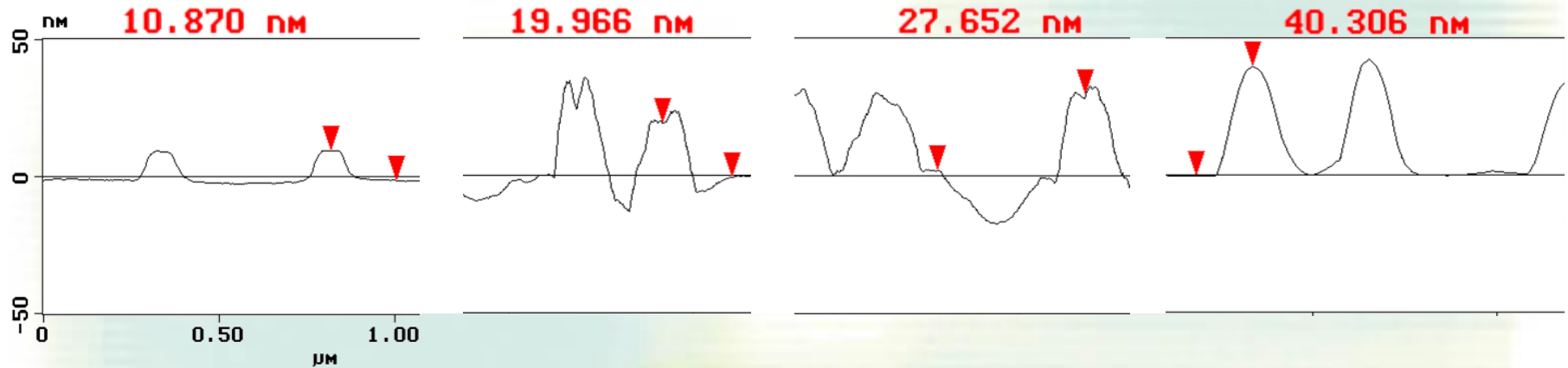


Fe_3O_4 deposition inside the nanocylinders

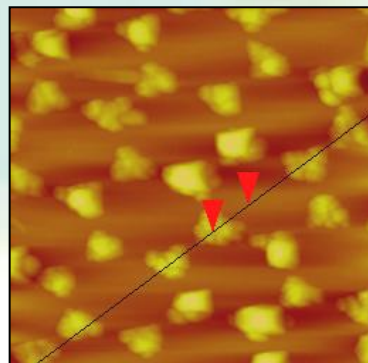


Transmission of light through magnetic nanocavities
Patoka P., et al. *Small* 7, 21, 3096-30100 2011

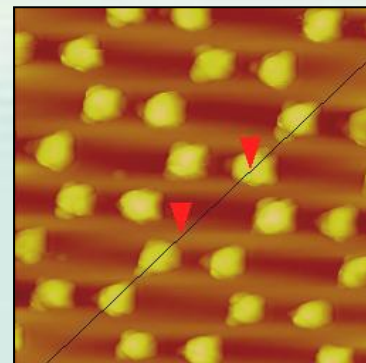
Modification of morphology



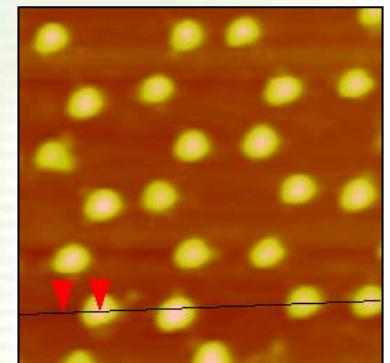
RT



750° C



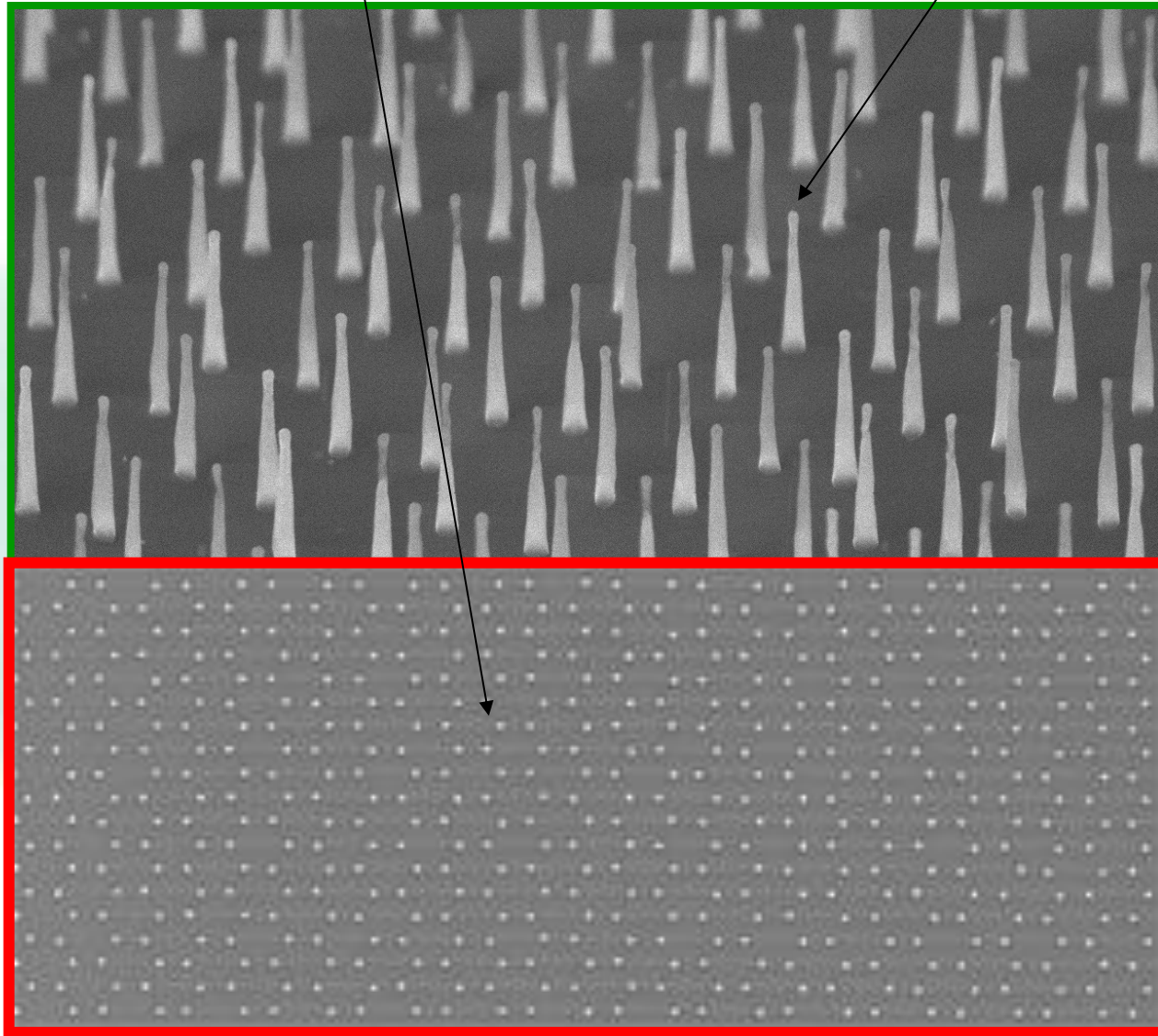
850° C



950° C

10 nm Ni evaporated through 496 nm latex beads mask after annealing for 50 min.

Application of nanocatalyst for growth of Carbon Nanotubes

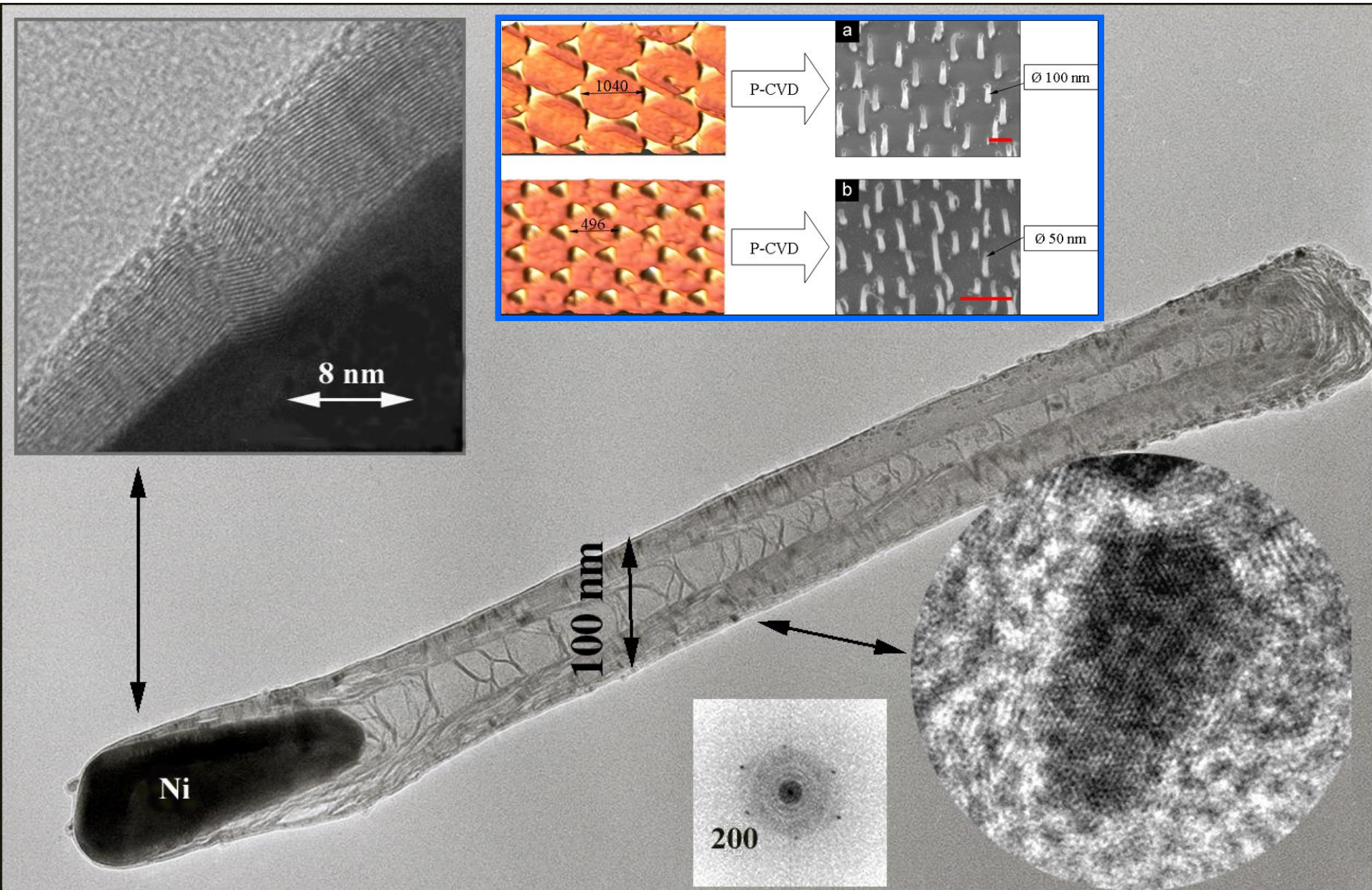


Multiwalled carbon nanotubes prepared in P-CVD from triangle-shaped 200 nm nickel particles

Kempa K., et al; NanoLetters 3, 13-18, 2002

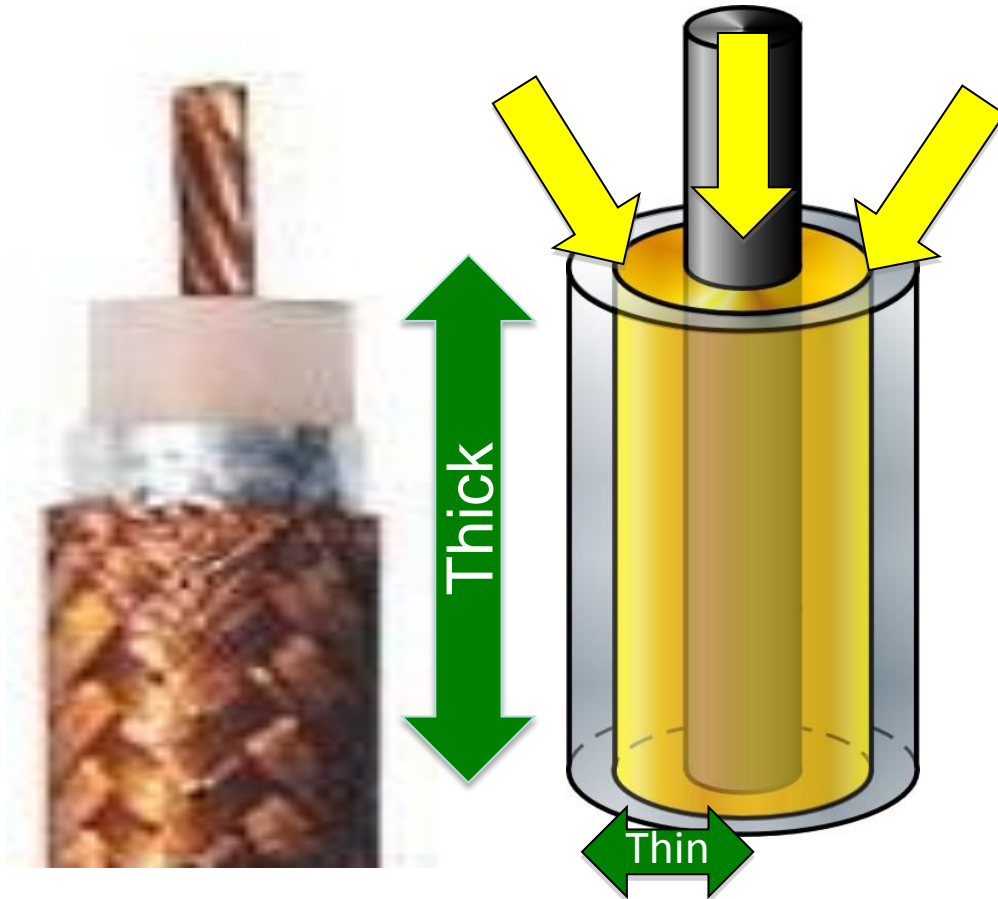
Rybczynski J., et al., Colloids and Surface; 219 1-6 2003

Photonic crystal based on Multiwall Carbon Nanotubes



Solar Cell

Nanocoax solar cell decouples photo- from -voltaic



Nanocoax Solar Cell:

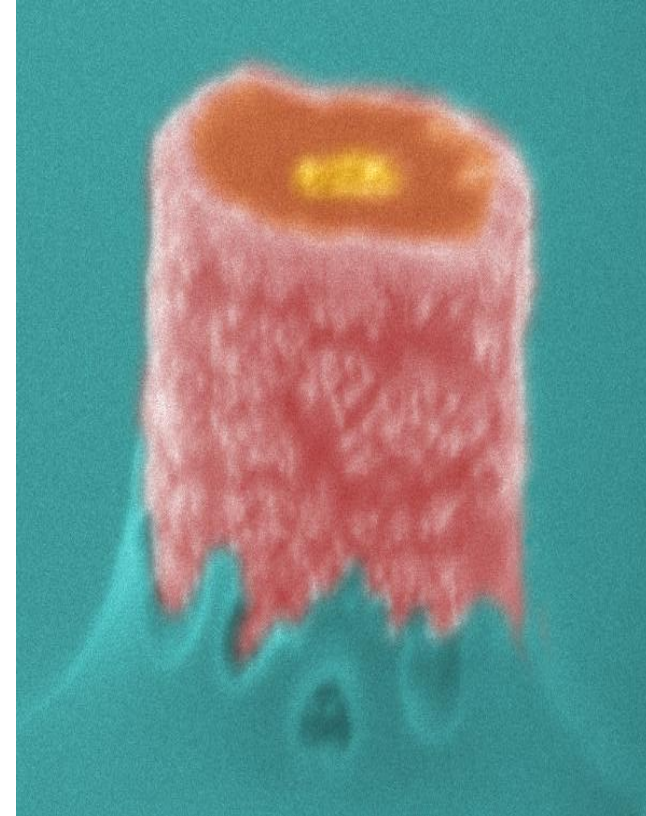
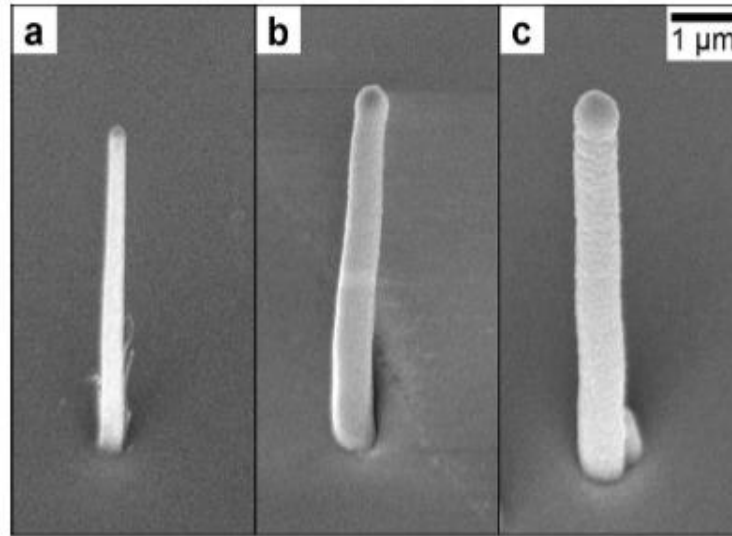
1. Antenna collection
2. Optically thick
3. Electronically thin



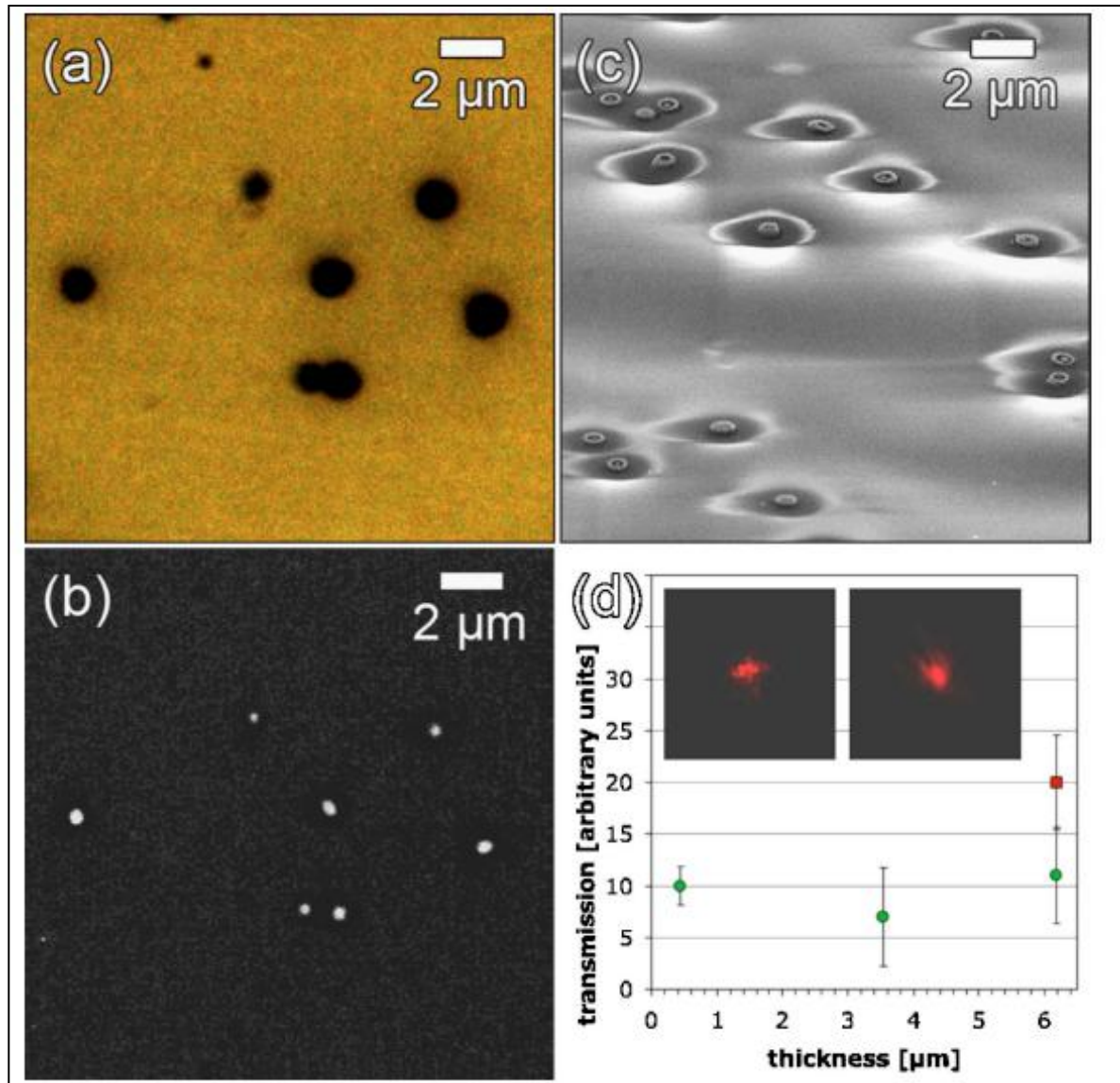
ultimate light trapping scheme, allowing ultrathin absorbers

Solar Cell

Nanocoax subwavelength waveguide for visible light

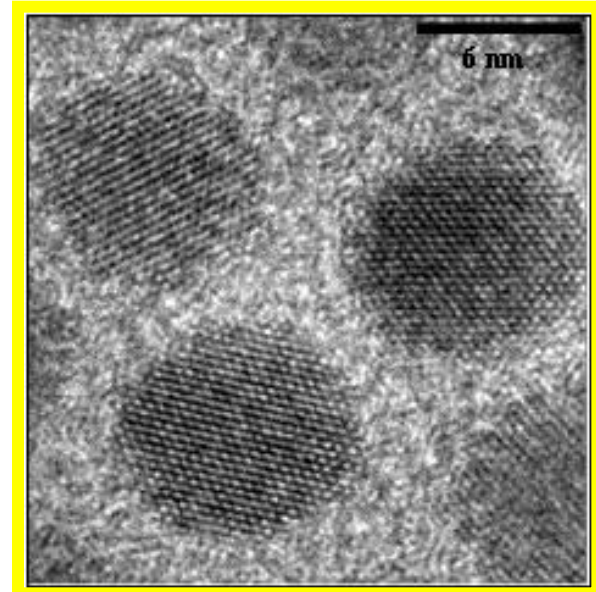
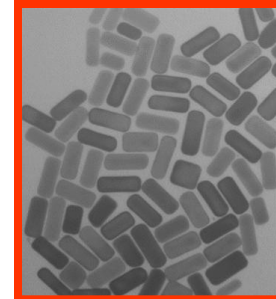
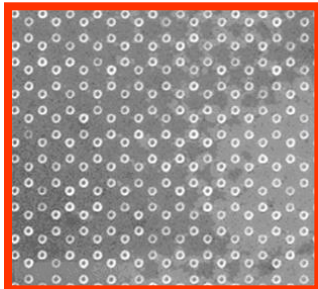
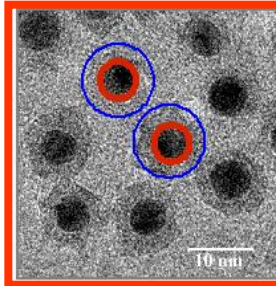
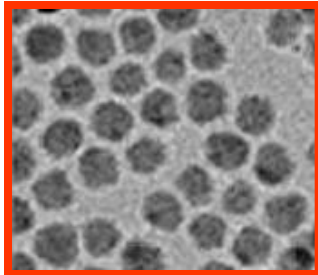
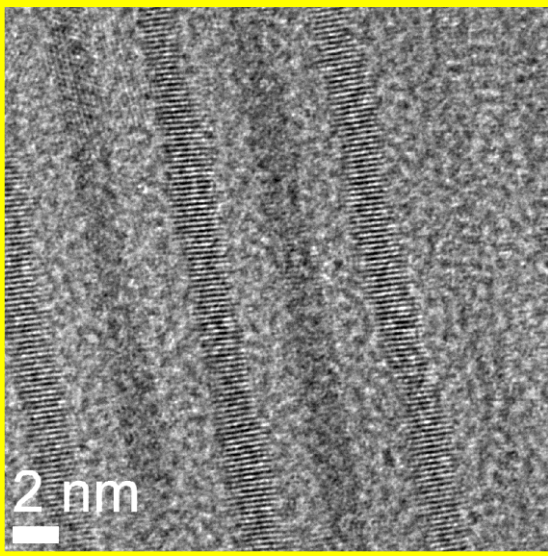
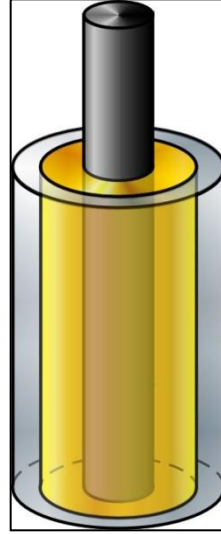


Nanocoax : subwavelength waveguide for visible light



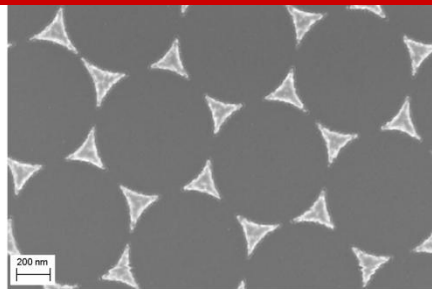
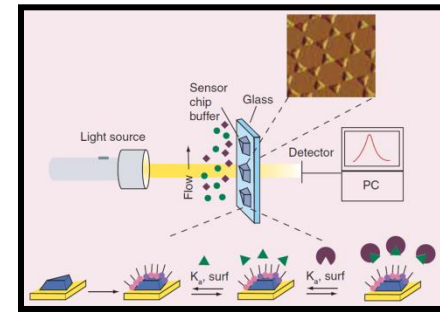
The third-generation of solar cells :Nanocoax Solar Cell

(high efficiency solar power requiring ultrathin absorbers)

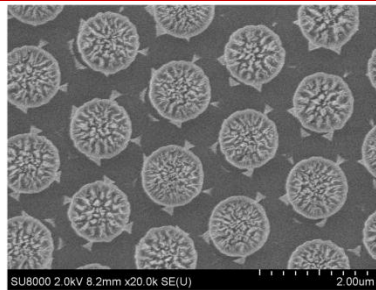


Outlook

Measurement of biosensing properties by Localized Surface Plasmon Resonance (LSPR) and Surface-Enhanced Raman Spectroscopy (SERS)



Mask deposition with NSL, etching



Evaporation of SiO₂ film, removal of PS nanospheres

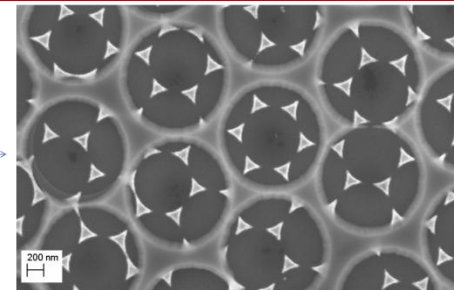
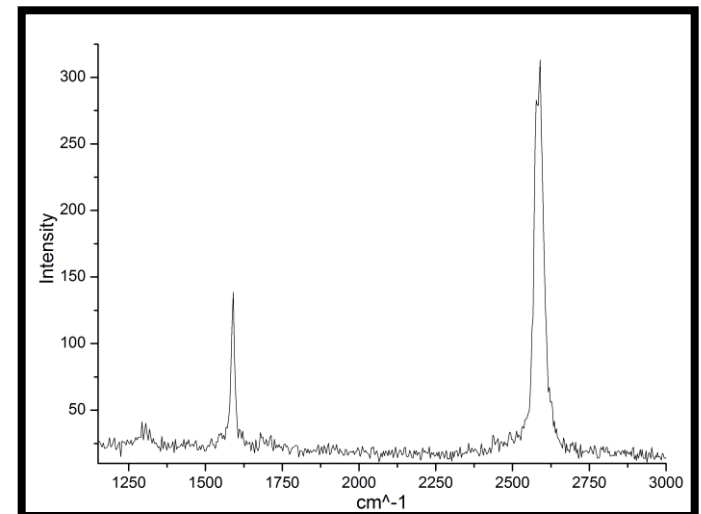
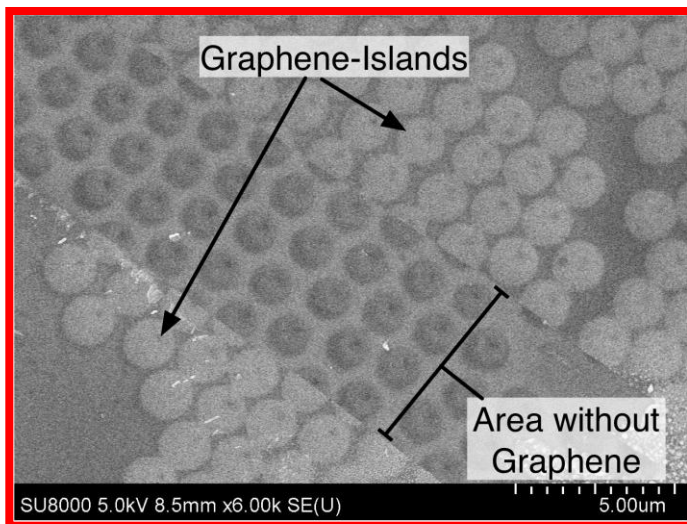


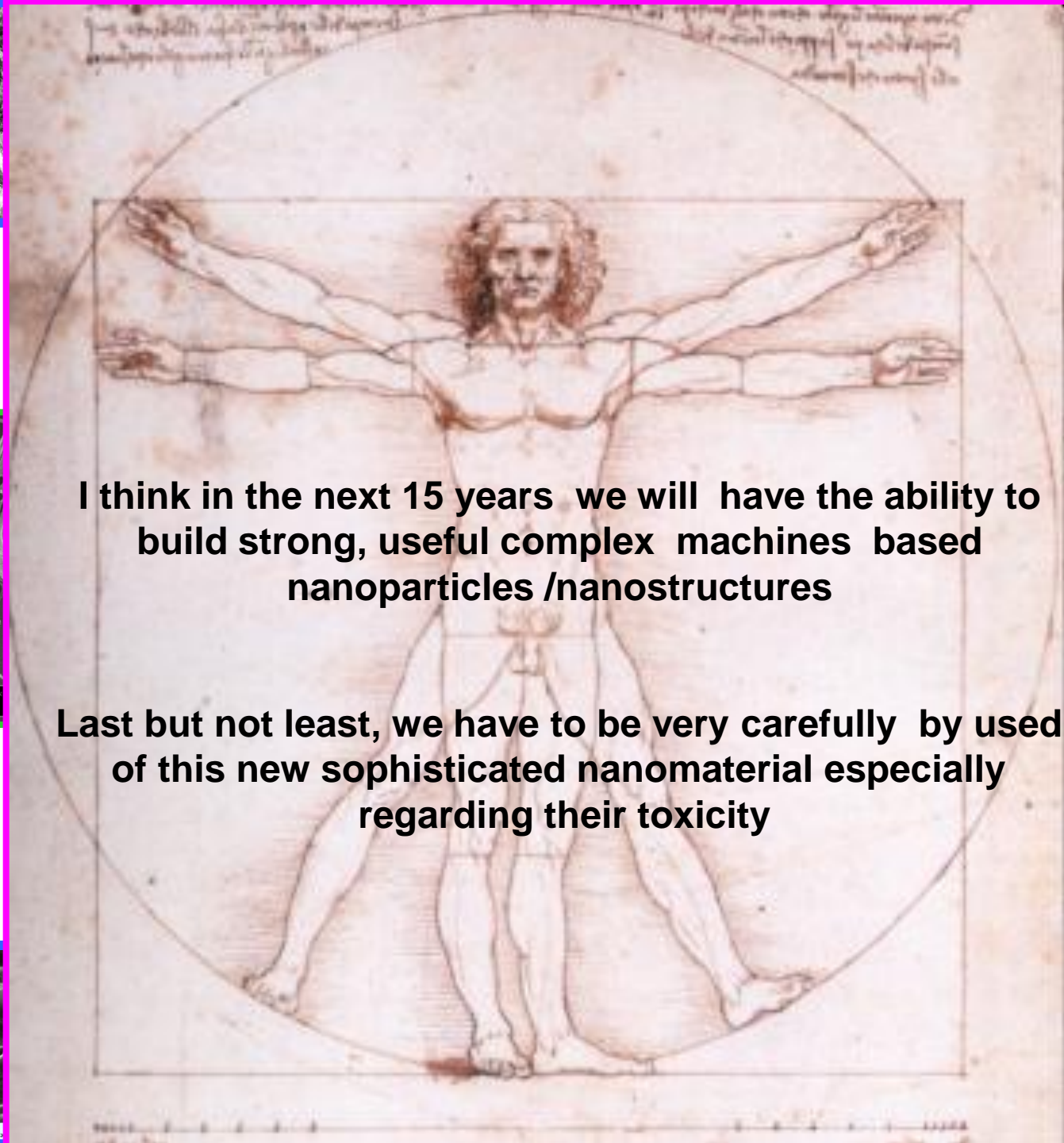
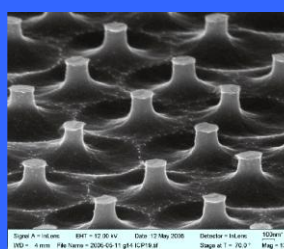
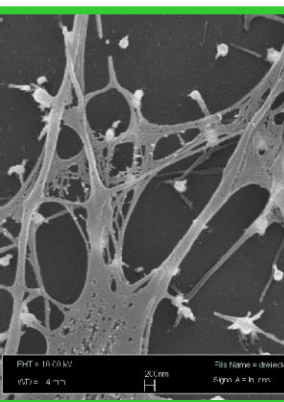
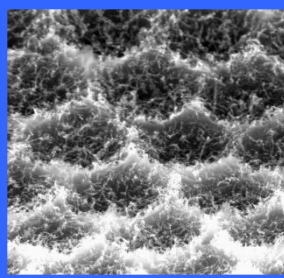
Fig.4 SEM image of array of golden nanoparticles deposited on silicon substrate in EBPVD process. Prepared with PS nanospheres of 756nm ϕ

Fig.5 SEM image of a mask of PS nanospheres deposited on an array of golden nanoparticles and etched afterwards. Prepared with PS nanospheres of 1300nm ϕ

Fig.6 SEM image of silicon dioxide film with an array of holes, on top of triangular gold nanoparticle array deposited on silicon substrate. The structure was obtained in EBPVD process.

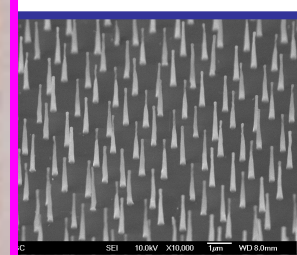
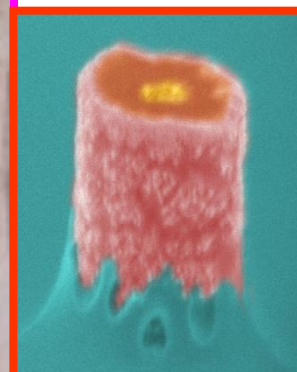
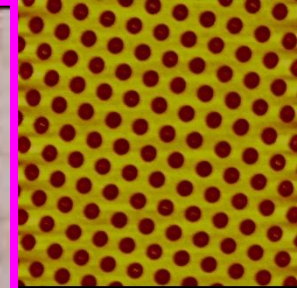
Low temperature CVD growth of Graphene





I think in the next 15 years we will have the ability to build strong, useful complex machines based nanoparticles /nanostructures

Last but not least, we have to be very carefully by used of this new sophisticated nanomaterial especially regarding their toxicity



ACKNOWLEDGMENTS TO COLLABORATORS / SUPPORT



Drs.

M. Hilgendorff

A. Morfa

P. Patoka

PhD

S. Haracz

E. Akinoglu

M. Legacz

Master.

N. Müller

V. Odone



Prof. K. Kempa

**Department Physics
Boston College**

Prof. P. Mulvaney

**School of Chemistry
University of Melbourne**

Prof. M. Antonietti

**Colloids and Surfaces
MPI- Golm**

Prof. D. Su

**Department of Inorganic
Chemistry, Fritz Haber
Institute of the Max
Planck Society Berlin**

Prof. L. Zhi

**Physical Chemistry
NTC Beijing**

Prof. B. Marciniak

**UAM Poznan
Dept. Physical Chemistry**

support from: FU-Berlin, HZB-Berlin, MPI-Golm, BMBF, EU